| Title | Attenuation of oxytocin and serotonin 2A receptor signaling through novel heteroreceptor formation |
|---|---|
| Author(s) | Chruścicka, Barbara; Wallace Fitzsimons, Shauna E.; Borroto-Escuela, Dasiel O.; Druelle, Clémentine; Stamou, Panagiota; Nally, Kenneth; Dinan, Timothy G.; Cryan, John F.; Fuxe, Kjell; Schellekens, Harriët |
| Publication date | 2019-04-30 |
| Original citation | Chruścicka, B., Wallace Fitzsimons, S. E., Borroto-Escuela, D. O., Druelle, C., Stamou, P., Nally, K., Dinan, T. G., Cryan, J. F., Fuxe, K. and Schellekens, H. (2019) 'Attenuation of Oxytocin and Serotonin 2A Receptor Signaling through Novel Heteroreceptor Formation', ACS Chemical Neuroscience, 10(7), pp. 3225-3240. doi: 10.1021/acschemneuro.8b00665 |
| Type of publication | Article (peer-reviewed) |
| Link to publisher's version | https://pubs.acs.org/doi/abs/10.1021/acschemneuro.8b00665 http://dx.doi.org/10.1021/acschemneuro.8b00665 Access to the full text of the published version may require a subscription. |
| Rights | **© 2019 American Chemical Society. This document is the Accepted Manuscript version of a Published Work that appeared in final form in ACS Chemical Neuroscience, copyright © American Chemical Society after peer review and technical editing by the publisher. To access the final edited and published work see https://pubs.acs.org/doi/abs/10.1021/acschemneuro.8b00665** |
| Embargo information | Access to this article is restricted until 12 months after publication by request of the publisher. |
| Embargo lift date | 2020-04-30 |
| Item downloaded from | http://hdl.handle.net/10468/8406 |

University College Cork, Ireland
Coláiste na hOllscoile Corcaigh

Article

# Attenuation of Oxytocin and Serotonin 2A Receptor Signalling through Novel Heteroreceptor Formation.

Barbara Chru#cicka, Shauna E Wallace Fitzsimons, Dasiel Oscar Borroto-Escuela, Clémentine Druelle, Panagiota Stamou, Kenneth Nally, Timothy G Dinan, John F Cryan, Kjell Fuxe, and Harriet Schellekens

## Just Accepted

# Attenuation of Oxytocin and Serotonin 2A Receptor Signalling through Novel Heteroreceptor Formation.

**Barbara Chruścicka[1,2], Shauna E. Wallace Fitzsimons[1,2], Dasiel O. Borroto-Escuela[4], Clémentine Druelle[1,2], Panagiota Stamou [1], Kenneth Nally[1], Timothy G. Dinan[1,3], John F. Cryan[1,3], Kjell Fuxe[4], Harriët Schellekens[1,2,*]**

[1]APC Microbiome Ireland, University College Cork, Cork, Ireland.

[2]Department of Anatomy and Neuroscience, University College Cork, Cork, Ireland.

[3]Department of Psychiatry and Neurobehavioural Science, University College Cork, Cork, Ireland

[4]Department of Neuroscience, Karolinska Institutet, Retzius väg 8, 17177 Stockholm, Sweden.

**Corresponding author**

[*]Harriët Schellekens, Department of Anatomy and Neuroscience, 3.85 Western Gateway Building, University College Cork, Cork, Ireland.

E-mail H.Schellekens@ucc.ie.

Tel +353 (0)21 420 54 29

## ABSTRACT

The oxytocin receptor (OTR) and the 5-hydroxytryptamine 2A receptor (5-HTR$_{2A}$) are expressed in similar brain regions modulating central pathways critical for social and cognition-related behaviours. Signalling crosstalk between their endogenous ligands, oxytocin (OT) and serotonin (5-hydroxytryptamine, 5-HT) highlights the complex interplay between these two neurotransmitter systems and may be indicative of the formation of heteroreceptor complexes with subsequent downstream signalling changes. In this study, we assess the possible formation of OTR-5HTR$_{2A}$ heteromers in living cells and the functional downstream consequences of this receptor-receptor interaction. First, we demonstrated the existence of a physical interaction between the OTR and 5-HTR$_{2A}$ *in vitro,* using a flow cytometry-based FRET approach and confocal microscopy*.* Furthermore, we investigated the formation of this specific heteroreceptor complex *ex vivo* in the brain sections using the Proximity Ligation Assay (PLA). The OTR-5HTR$_{2A}$ heteroreceptor complexes were identified in limbic regions (inter alia hippocampus, cingulate cortex, and nucleus accumbens), key regions associated with cognition and social-related behaviours. Next, functional cellular-based assays to assess the OTR-5HTR$_{2A}$ downstream signalling crosstalk showed a reduction in potency and efficacy of OT and OTR synthetic agonists, carbetocin and WAY267464 on OTR-mediated G$\alpha$q signalling. Similarly, the activation of 5-HTR$_{2A}$ by the endogenous agonist, 5-HT, also revealed attenuation in G$\alpha$q-mediated signalling. Finally, altered receptor trafficking within the cell was demonstrated, indicative of co-trafficking of the OTR/5-HTR$_{2A}$ pair. Overall, these results constitute a novel mechanism of specific interaction between the OT and 5-HT neurotransmitters via OTR-5HTR$_{2A}$ heteroreceptor formation and provide potential new therapeutic strategies in the treatment of social and cognition-related diseases.

**KEYWORDS:** OTR, 5-HTR$_{2A}$, heteroreceptor complexes, fcFRET, PLA, G$\alpha$q-mediated signalling crosstalk

## INTRODUCTION

Oxytocinergic signalling represents one of the major neuroendocrine systems in mammals [1]. Oxytocin (OT), a nine-amino acid peptide hormone, is produced in paraventricular (PVN) and supraoptic nuclei of the hypothalamus. Peripherally-secreted OT is mainly known to stimulate uterine smooth muscle contractions associated with parturition and milk ejection during lactation [2–5]. The known actions of OT are mediated through the OT receptor (OTR), which belongs to the largest subclass of the rhodopsin-β adrenergic receptor family (class A) of G-protein coupled receptors (GPCRs) [6,7]. Detection of OTR in kidney, thymus, bone cells, osteoblasts, cardiomyocytes, vascular endothelial cells and different types of cancer cells highlights the vast spectrum of peripheral OT functionalities from fertility regulation to controlling the immune and cardiovascular systems, bones and muscles formation, and growth of certain cancer cells [8–10].

Within the central nervous system, OT is released in a number of brain regions, including limbic structures and sensory processing areas, where this peptide functions as a neurotransmitter [11,12]. Central OT has been found to primarily modulate complex social and cognitive behaviours, such as; social memory, recognition and reward, attachment, cooperation, exploration, motivation, as well as anxiety and aggression [13–16]. Furthermore, dysfunction in the OT system is associated with several mental disorders characterized by social impairments, including autism spectrum disorders (ASD), social anxiety disorder and schizophrenia [17,18]. Many pre-clinical and clinical data have shown beneficial effects of OT administration on social cognition and prosocial behaviour [14,19,20]. The promising therapeutic potential of exogenous OT on social related behaviours was demonstrated across multiple studies in healthy subjects as well as in patients with ASD and schizophrenia [21,22]. However, an increasing number of studies is also showing evidence of inconsistent effects of exogenous OT administration between subjects, especially in patients with ASD and schizophrenia [23–25]. These variable OT responses, highlight that the efficacy of the OT administration in human has not yet been firmly established [26–28]. The differences in effects between subjects may be explained by the complex nature of the OT signalling system, as well as different basal levels of neurotransmitters in specific brain regions. This may suggest that the OT system is able to interact with multiple

neurotransmitters, modulating social related behaviours through different mechanisms, which influence the final functional outcome [29–31].

The ability of OT to modulate the serotonin (5-hydroxytryptamine, 5-HT) system have been demonstrated across multiple studies [31–34]. Serotonergic projections innervate almost every brain region, and 5-HT represents the key neurotransmitter involved in several behaviours including, mood, stress, and social behaviours [35,36]. Interestingly, OT administration has been shown to significantly increase 5-HT axon length and density in the amygdala and hypothalamus of prairie vole males during development, demonstrating OT-mediated modulation of 5-HT innervation in early life [33]. The OT neuropeptide is also known to influence 5-HT synthesis and release from 5-HT neurons in the midbrain raphe nuclei, leading to a reduced anxiety-like behaviour in mice [32]. The modulation of 5-HT release by the OT peptide is driven through OTR and serotonin 2A/2C receptors (5-HTR$_{2A/2C}$), which are both expressed on 5-HT neurons. Interestingly, 5-HT receptors, including the 5-HTR$_{2A/2C}$, have been shown to mediate OT secretion from the PVN of the hypothalamus [37–39]. In addition, several studies have demonstrated the impact of elevated plasma 5-HT, as seen in one-third of ASD patients, on OT system dysregulation in a developmental hyperserotoninemic model. Hyperserotonemic rodents were characterized by a decreased number of OT expressing cells in the PVN, which was correlated with significantly lower expression of the 5-HTR$_{2A}$ on these neurons [40–42]. Recent studies have yielded very exciting results, demonstrating that the coordinated activity of OT and 5-HT neurotransmitters in the nucleus accumbens of mice is crucial for the rewarding properties of social interactions [31]. This specific interaction between OT and 5-HT systems was then validated in nonhuman primates and in humans, where OT administration influenced 5-HT signalling in the amygdala, insula, hippocampus, dorsal raphe nucleus, and orbitofrontal cortex, key limbic regions implicated in the control of stress, mood, and social behaviours [29,34]. Although the OTR and 5-HTRs have been suggested to be involved in behaviours listed above, the precise mechanism of the neurotransmitter system interaction has not yet been fully elucidated. Nevertheless, evidence is emerging highlighting a specific crosstalk between the OT and 5-HT neurotransmitter systems, with a particular role for the OTR and 5-HTR$_{2A}$.

Similarly to the OTR, the 5-HTR$_{2A}$ also belongs to class A GPCRs, being primarily coupled to Gαq proteins following its activation [43,44]. Both GPCRs are critical signal

4

transducers in the brain and have received much attention as promising therapeutic targets for social and cognition related disorders [45–47]. In addition, both OTR and 5-HTR$_{2A}$ are well known to crosstalk with other GPCRs through formation of heteroreceptor complexes [48–51]. Oligomerization of GPCRs is known to modulate their downstream signalling and exert a significant impact on receptor physiology and function [48,52–54]. Interestingly, the changes in the formation and function of GPCRs heterodimers are associated with many neuropsychiatric disorders [55–58]. For example, formation of an OTR/dopamine 2 receptor (D2R) heteroreceptor complex has been shown to affect downstream signalling of both receptors and modulate the OT-mediated anxiolytic effect [49,53,59]. Downstream signalling of the 5-HTR$_{2A}$ in complexes with the D2R and the metabotropic 2 receptor (mGluR2) have also been shown to be affected [48,57]. Furthermore, the formation of such specific 5-HTR$_{2A}$ heteroreceptor complexes has been implicated in the mechanism of antipsychotic and hallucinogenic drugs actions [55,60,61]. The mechanism of atypical antipsychotics is also a good example that compounds interacting simultaneously with multiple GPCRs are clinically more effective, compared to drugs specific for one receptor [62]. Identification and characterization of novel crosstalk and heteromerization between different GPCRs are poised to yield promising future pharmacotherapeutic strategies for the development of novel drug with high efficacy and specificity for many central nervous system (CNS) disorders, especially for those with a multifactorial and polygenic aetiology.

Based on the reciprocal interaction of the OT and 5-HT systems, and the fact that both the OTR and 5-HTR$_{2A}$ are involved in social and cognition related behaviours with an overlapping central expression profiles within brain regions associated with these processes, we hypothesize that the OTR and 5-HTR$_{2A}$ may form heteroreceptor complexes. In this study, we first evaluate the possible formation of OTR-5HTR$_{2A}$ heterororeceptor complexes *in vitro* using a flow cytometry-based FRET (fcFRET) approach and confocal microscopy. Next, the formation of these specific heteroreceptor complexes is investigated *ex vivo*, in rat brain sections with the use of Proximity Ligation Assay (PLA) [63]. Finally, functional cellular-based assays, including intracellular calcium mobilization, IP-One accumulation and ligand-mediated trafficking [54,64] are used to demonstrate the significant changes in the G$\alpha$q-dependent signalling and trafficking of both receptors. Overall, these data show for the first time convincing evidence for the formation of the OTR-5HTR$_{2A}$ functional heteroreceptor

complex, which may represent a novel molecular mechanism underpinning the OT and 5-HT signalling system crosstalk in the brain.

6

## RESULTS AND DISCUSSION

**Flow cytometry-based FRET demonstrates a physical interaction between the OTR and 5-HTR$_{2A}$.**

The interaction between the OTR and 5-HTR$_{2A}$ was assessed in human embryonic kidney (HEK293A) cells expressing the receptors under investigation using flow cytometry-based FRET (fcFRET). The fcFRET analysis allows the evaluation of the physical interactions between receptors in a large population of cells, providing statistically more robust and reliable data compared to confocal microscopy. In addition, this method classifies the population of cells and elucidates the difference in fcFRET efficiency with other cellular parameters, such as; viability, size and granulation [51]. Indeed, fcFRET is a non-invasive, sensitive and quantitative method that has been successfully used to assess protein-protein interactions, including the physical interaction between GPCRs [66–68].

To optimize an assay for quantitative measurements of fcFRET signal HEK293A cells with the expression of fluorescent protein tags (tGFP and tRFP), without any GPCRs were first analysed. Analysis of fcFRET signal was performed on the gated population of single, live, and successfully transduced cells. As expected, cells containing both fluorescent proteins (HEK293A-tGFP-Lv-tRFP) did not show a significant fcFRET signal and neither did cells expressing each tag separately or HEK293A cells without tags (Figure 2, supplementary data). This result indicates that the fcFRET signal detected between receptors under investigation is not due to an overexpression, random collision or dimerization of fluorescent proteins. Next, we demonstrated a significantly higher fcFRET signal in cells co-expressing the OTR tagged with tGFP and OTR tagged with tRFP (HEK293A-OTR-tGFP-Lv-OTR-tRFP) (28.8 ± 1.5%) when compared to cells expressing either the OTR tagged with tGFP (0%), or OTR tagged with tRFP (0.2 ± 0.2%) (Figure.1 supplementary data). In addition, cells with the expression of the donor construct and the control acceptor construct (HEK293A-OTR-tGFP-control-tRFP) were used for quantification of nonspecific fcFRET signal (1.4 ± 0.4%) [66]. These results confirmed the ability of the OTR to form constitutive homodimers [50,69] and showed the reliability of the experimental settings.

Next, analysis of fcFRET signal between the OTR and 5-HTR$_{2A}$ receptors was performed. A significant increase in the percentage of fcFRET positive cells was observed for cells co-expressing 5-HTR$_{2A}$-EGFP and OTR-tRFP (HEK293A-5HTR$_{2A}$-

7

EGFP-Lv-OTR-tRFP) (23.3 ± 3.1%) compared to cells solely expressing the donor construct (HEK293A-5HTR$_{2A}$-EGFP) (0.3 ± 0.03%) or acceptor construct (HEK293A-Lv-OTR-tRFP) (0.3 ± 0.03%) and compared to cells expressing the 5-HTR$_{2A}$-EGFP with control-tRFP construct (3.2 ± 0.6%) (Figure 1A and 1C). Furthermore, fcFRET signal analysed as median fluorescence was also significantly higher in cells co-expressing the OTR/5-HTR$_{2A}$ pair (48 ± 1.6 RFU) compared to cells with the expression of the donor (15,3 ± 5.2 RFU) or acceptor (18,7 ± 10.3 RFU) construct only and compared to cells expressing the 5-HTR$_{2A}$-EGFP with the control-tRFP construct (14.2 ± 6.9 RFU) (Figure 1B and 1D). Taking together, the above results highlighted the constitutive and specific association between the OTR and 5-HTR$_{2A}$ within the cell, indicating the formation of a heteroreceptor complex between these receptors *in vitro*, in intact HEK293A cells.
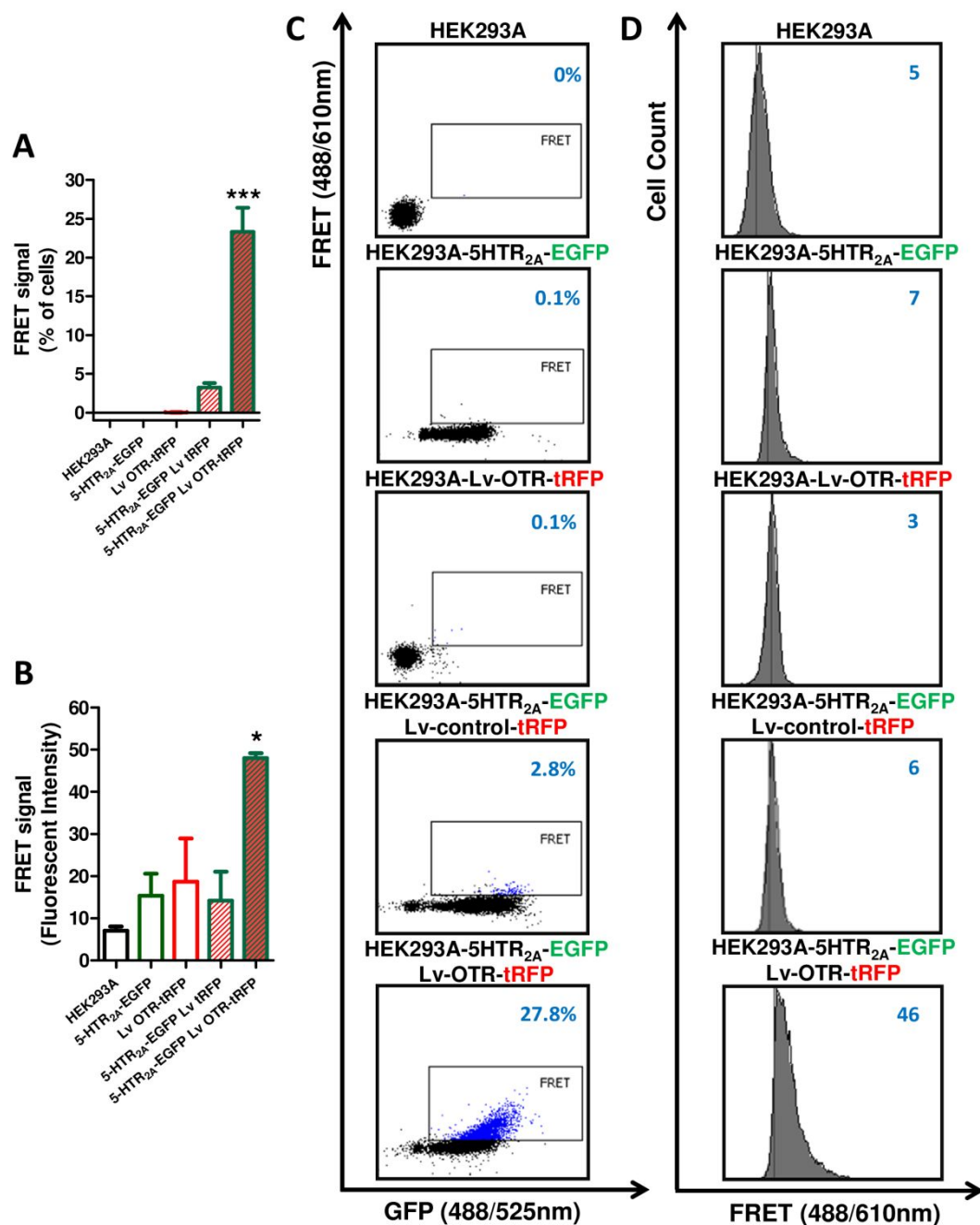
**Figure 1. fcFRET between the OTR and 5-HTR$_{2A}$.** The fcFRET signal is presented as a percentage of cells (A,C) and as median fluorescence (B,D) in wild-type HEK293A cells, cells stably expressing the 5-HTR$_{2A}$ tagged with EGFP (donor), cells transiently transduced with lentiviral vector expressing OTR tagged with tRFP (acceptor), cells expressing 5-HTR$_{2A}$ tagged with EGFP and the control-tRFP, and cells co-expressing 5-HTR$_{2A}$ tagged with EGFP and OTR tagged with tRFP. Graphs represent mean ± SEM from three independent experiments (A,B). Statistical significance of fcFRET signal in cells co-expressing both receptors compared to cells expressing donor with the control acceptor constructs is denoted as * for $p < 0.05$ and *** for $p < 0.001$. Dot plots (C) show percentage of cells with fcFRET signal (FRET vs EGFP plots), histograms (D) demonstrate median fluorescence of fcFRET signal (Cell count vs FRET signal). Dot plots and histograms are representative of three independent experiments.

**Cellular colocalization of the OTR and 5-HTR$_{2A}$.**

9

Cellular localization of the receptors was investigated using a confocal microscopy in intact living HEK293A cells co-expressing the OTR and 5-HTR$_{2A}$. The 5-HTR$_{2A}$ was mainly found within the cell membrane which was shown by the green fluorescence signal from 5-HTR$_{2A}$ fused with EGFP (Figure 2A). The red fluorescence signal from OTR fused with tRFP was shown on the cell membrane, as well as in the intracellular space (Figure 2B). The ubiquitous expression of the OTR-tRFP within the cell may be explained by constitutive (ligand-independent) activity and internalization of the OTR, as well as the previously described low rate of recycling back to the cell membrane [70,71]. Moreover, a similar pattern of OTR expression is observed in a number of heterologous expression systems as well as endogenously in different type of tissues [72–75] (also see Figure 3 in supplementary data). Interestingly, an overlap between green and red fluorescence as indicated by the yellow signal demonstrated colocalization of both receptors on the cell membrane and within the cytoplasm of cells (Figure 2C, merged picture). The colocalization of the OTR/5-HTR$_{2A}$ pair within the same confocal plane is evidence for the potential formation of OTR-5-HTR$_{2A}$ heteromers and reinforces the observed fcFRET signal (Figure 1). What is more interesting colocalization between the OTR and 5-HTR$_{2A}$ observed intracellularly may indicate possible co-trafficking of both receptors within the cell, which was previously observed in the case of other GPCRs heterodimer pairs [64,76,77].
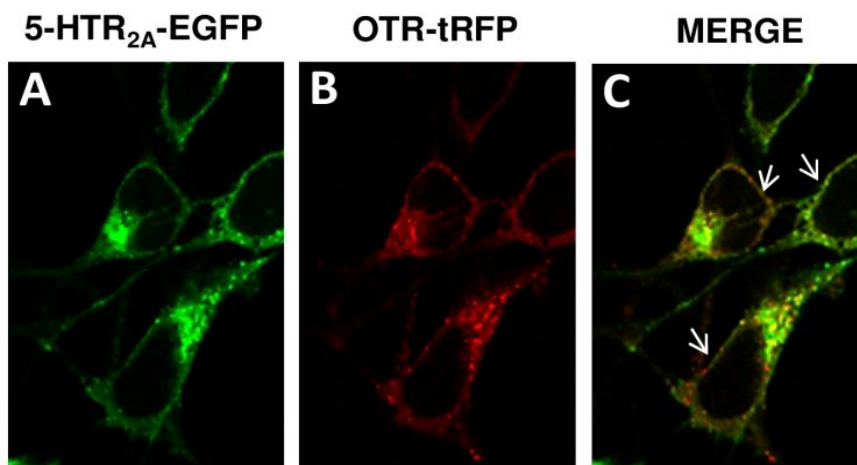


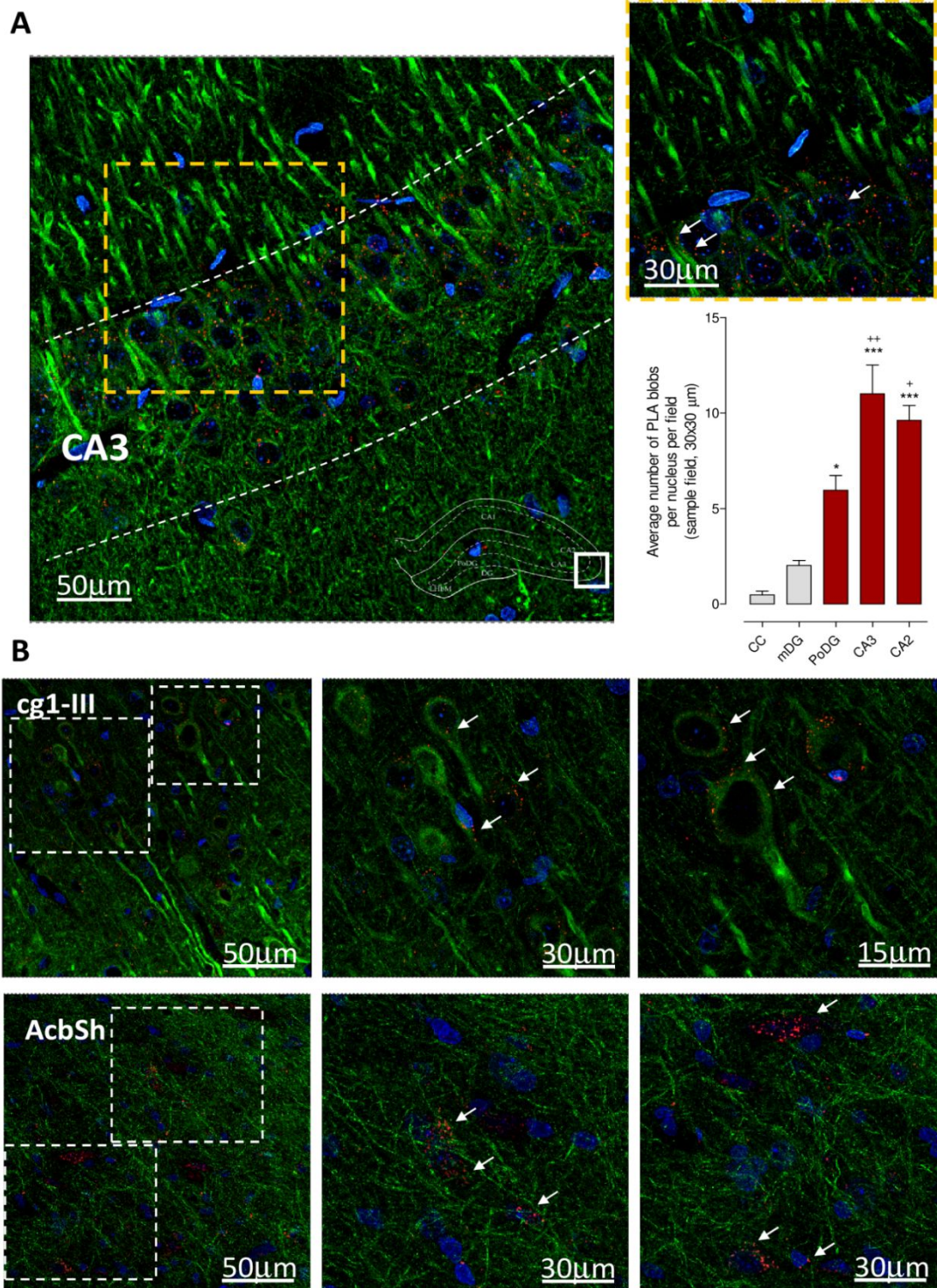**Figure 2. Cellular colocalization of the OTR/5-HTR$_{2A}$ pair.** HEK293A cells stably expressing the 5-HTR$_{2A}$ tagged with EGFP (green) (A) were transiently transduced with lentiviral vector expressing OTR tagged with tRFP (red) (B). Merged picture (yellow/orange) shows colocalization of the two receptors within the cell (C).

**The OTR and 5-HTR$_{2A}$ form heteroreceptor complexes in rat brain regions.**

In the dorsal hippocampus of WT SD rats (Bregma -3.6 mm) a high density of PLA positive OTR-5HTR$_{2A}$ heteroreceptor complexes clusters was found in the pyramidal cell layer of the CA2 and CA3 regions, while only a few were found in the stratum oriens and radiatum of these areas. This was similar to the background found in negative controls and the myelinated bundles of the crus cerebri (CC) (Figure 3A). A multiple z-scan (20) confocal microscopy photograph corresponding to the CA3 region with higher magnification of the high-density PLA positive clusters is shown in Figure 3A. The quantitative data present the number of PLA clusters (blobs) per nucleus per sampled field (30X30 μm). They range mainly from 8-13 PLA clusters in the CA2 and CA3 regions to 4-6 PLA clusters in the polymorphic layer of the dentate gyrus (PoDG) and it shows the high density in the pyramidal cell layer. A very low density of the PLA clusters is found in the granular cell layer of the dentate gyrus (gDG). The molecular cell layer of the dentate gyrus (mDG) contains densities similar to the densities and values found in negative controls.

In the cingulate cortex (Bregma 1.2 mm) a PLA positive OTR-5HTR$_{2A}$ heteroreceptor complexes clusters is found in layers II and III, shown in low and high magnifications (Figure 3B). Also, a PLA positive clusters was found in the nucleus accumbens shell and core (Bregma 1.2 mm) (Figure 3B). In the dorsal striatum these receptor complexes could not be clearly observed.

A PLA positive signal validates the *in vitro* results and demonstrates the formation of OTR-5HTR$_{2A}$ heteroreceptor complexes in rat brain sections under endogenous expression levels of both receptors. Moreover, specific distribution pattern of OTR-5HTR$_{2A}$ heteroreceptor complexes indicate their potential role in distinct cortical and subcortical limbic regions. The formation of these receptor complexes in the CA2 and CA3 regions of the hippocampus and cingulate cortex may be involved in modulation of OTR dependent social recognition and memory [20] as well as 5HTR$_{2A}$ driven social exclusion processing [78]. It is also tempting to hypothesize that OTR-5HTR$_{2A}$ heteromers identified in nucleus accumbens can be partially responsible for the crosstalk between OT and 5-HT neurotransmitters shown to be crucial for rewarding properties of social interactions [31]. In conclusion, the above results underlie the potential role of OTR-5HTR$_{2A}$ heteroreceptor complexes in distinct limbic circuits relevant to social interactions.

**Figure 3. Illustration of the OTR-5HTR$_{2A}$ heteroreceptor complexes in the dorsal hippocampus and nucleus accumbens of rat brain.** (A) Microphotographs from transverse sections of the rat dorsal hippocampus (Bregma level: -3.6 mm) show the distribution of the OTR-5HTR$_{2A}$ heteroreceptor complexes in CA3 using the *in situ* proximity ligation assay (*in situ* PLA) technique. The square outlines the CA3 area from which the picture was taken. Receptor complexes are shown as red PLA blobs (clusters) found in high densities per cell in a large number of nerve cells in the pyramidal cell layer using confocal laser microscopy. No specific PLA blobs were found in the stratum moleculare and radiatum of the CA3-CA2 regions (*cornus ammonis*). The nuclei are shown in blue by DAPI staining and the neuronal marker in green

(Neuro-Chrom™ Pan neuronal marker antibody-Alexa488 conjugated, ABN2300A4). In the higher right panel the PLA blobs are presented in higher magnification in the pyramidal cell layer. In the lower right part of the figure the density (per nucleus per sampled field) of the PLA positive complexes in PoDG (polymorph layer of the dentate gyrus), CA3, and CA2 are highly significantly different (***) from the density found in crus cerebri (CC) and the granular cell layer of the dentate gyrus (gDG). The density is also significantly higher in the CA2 (+) and CA3 (++) versus PoDG (Mean ± SEM, 4 rats per group). (B) The upper panel of B show representative examples of these PLA receptor complexes from transverse sections of the rat cingulate cortex, area 1 (Bregma level: 1.2 mm). They present the distribution of OTR-5HTR$_{2A}$ heteroreceptor complexes. They are shown as red PLA blobs (clusters) in layers II and III. Layer III represents the external pyramidal cell layer where large PLA positive clusters are found and appear to be located on the surface of many pyramidal cells. Higher magnifications of the two squares outlined in left panel are shown in the two right panels. The nerve cell bodies and apical dendrites are seen in green (neuronal marker). The lower panel in B is taken from nucleus accumbens shell (AcbSh). The neuronal marker (Neuro-Chrom™ Pan neuronal marker antibody-Alexa488 conjugated, ABN2300A4) shows the neurite network. A number of nerve cell bodies are associated with a PLA positive blobs representing OTR-5HTR$_{2A}$ heteroreceptor complexes that may also have an intracellular location through trafficking. The outlined squares in the left panel are shown in higher magnifications in the two right panels (B).

**Ligand-mediated internalization of the OTR and 5-HTR$_{2A}$.**

Desensitisation and subsequent internalization of GPCRs provides an important physiological mechanism that protects cells against overstimulation [73,79,80]. Most GPCRs, including the OTR and 5-HTR$_{2A}$ are rapidly internalized following agonist treatment and efficiently recycle to the cell surface after agonist removal [71,79–81]. It has been documented that the formation of heteroreceptor complexes can affect basal and ligand-mediated internalization of the heterodimer protomers within the cell [64,76,82]. Thus, we investigated the effect of co-expression of the OTR and 5-HTR$_{2A}$ on their cellular trafficking under basal conditions and following treatment with their respective endogenous ligands, oxytocin (OT) (100 nM) and serotonin (5-HT) (1 µM) (Figure 4). Significant OT-mediated internalization of the OTR tagged with tRFP was observed in cells solely expressing the OTR (HEK293A-Lv-**OTR-tRFP**) (Figure 4A). Similarly, significant internalization of the 5-HTR$_{2A}$ tagged with EGFP was shown following 5-HT treatment in cells solely expressing the 5-HTR$_{2A}$ (HEK293A-**5HTR$_{2A}$-EGFP**) (Figure 4B). Interestingly, in cells co-expressing both receptors (HEK293A-5HTR$_{2A}$-EGFP-Lv-**OTR-tRFP**), a significant increase in basal internalization of the OTR was observed. Further increase in OT or 5-HT-mediated internalization compared to control conditions although small also was noted in these cells (Figure 4A, blue bars with stripes). Moreover, we observed that the basal internalization of the 5-HTR$_{2A}$ in cells co-expressing both receptors (HEK293A-**5HTR$_{2A}$-EGFP**-Lv-OTR-tRFP) was consistently increased compared to cells solely expressing the 5-HTR$_{2A}$ (Figure 4B).

Interestingly, when both receptors were co-expressed (HEK293A-5HTR2A-EGFP-Lv-OTR-tRFP) a small, albeit insignificant increase in 5-HTR$_{2A}$ internalization was consistently observed following OT treatment compared to the control condition (untreated cells) (Figure 4B).

Changes in basal trafficking properties of the OTR and 5-HTR$_{2A}$ following their co-expression in mammalian cells may at least partially explain the colocalization of both receptors observed not only on the subcellular membrane but also intracellularly (Figure 2C). Moreover, these observations are similar to what was shown for the 5-HTR$_{2A}$ and the metabotropic glutamate receptor 2 (mGluR2) [60]. These receptors demonstrated to form stable 5-HTR$_{2A}$-mGluR2 heterodimers in HEK293 cells, which significantly increased their intracellular presence under basal conditions. This indicates that both receptors are assembled as heterocomplexes at an early stage, during maturation and trafficking to the cell membrane [77]. Several other studies have shown that GPCRs are indeed secreted to the cell surface as oligomerized complexes [50,83,84]. Thus, the significant intracellular presence of the OTR and 5-HTR$_{2A}$ following their co-expression in cells may suggest that OTR and 5-HTR$_{2A}$ also form constitutive heteromers during maturation and trafficking from endoplasmic reticulum to the cell membrane. Alternatively, the above results may indicate an increase in basal activity of both receptors and a subsequent higher internalization rate as previously shown for cannabinoid CB1 and orexin OX$_1$ receptor complexes [76]. Noteworthy, the increased internalization of the 5-HTR$_{2A}$ after treatment with OT may support the hypothesis that the 5-HTR$_{2A}$ is co-internalized along with the OTR, from the cell membrane to membranes of the endosomal compartment as previously demonstrated for the 5-HTR$_{2A}$-mGluR2 and the 5-HTR$_{2C}$-GHSR1a heteromers [60,64]. The OT-induced changes in cellular trafficking of the 5-HTR$_{2A}$ are also consistent with the formation of stable OTR-5-HTR$_{2A}$ heteromer complexes demonstrated in Figure 1.

Finally, the changes in basal and ligand-mediated cellular receptor trafficking may also lead to alterations in the downstream signalling pathways of each protomer. This may be particularly relevant for increased signalling over the β-arrestin pathway, which not only leads to an increased receptor internalization [85] but also directly affects the G protein-dependent downstream signalling pathways of GPCRs [86].
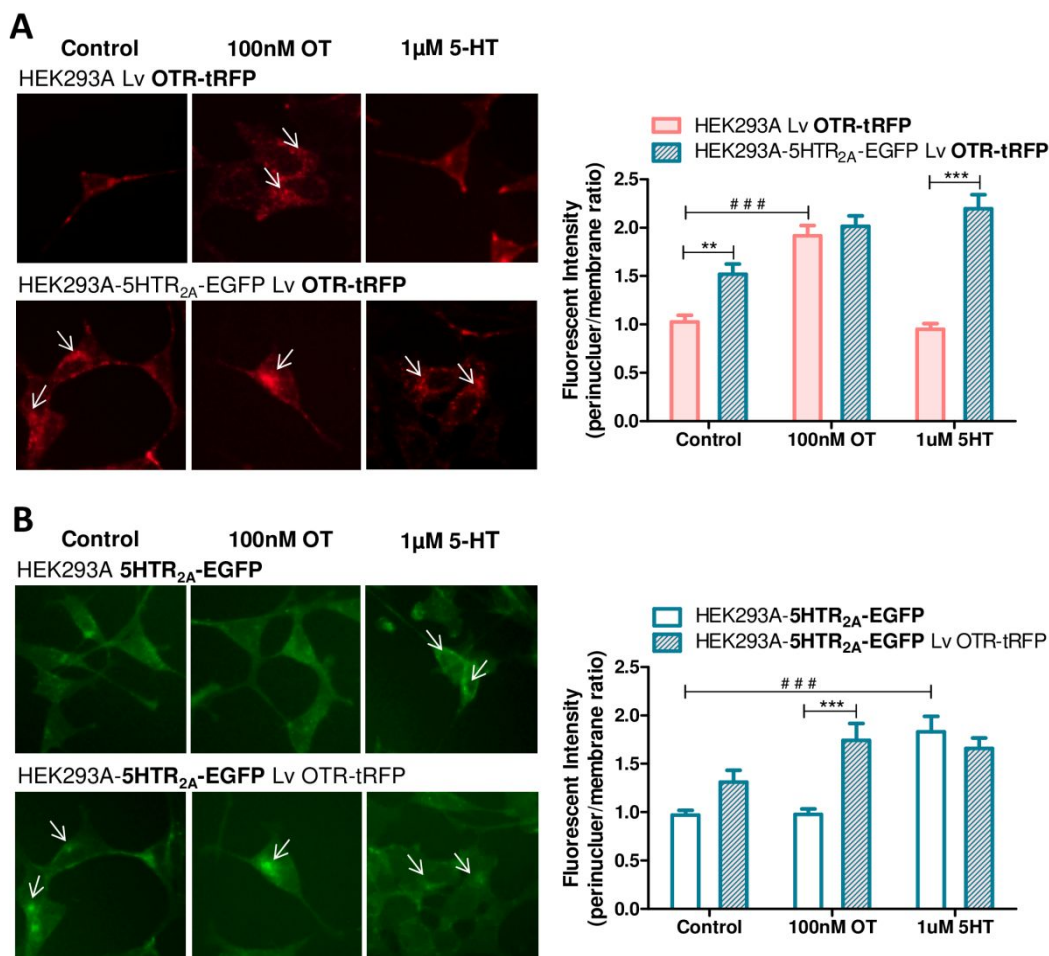
**Figure 4. Cellular trafficking of the OTR and 5-HTR$_{2A}$.** Representative images (left panel) and quantitative analysis (right panel) of ligand-mediated internalization of OTR tagged with tRFP (A) and 5-HTR$_{2A}$ tagged with EGFP (B) versus cells co-expressing both receptors. Graphs represents mean ± SEM from three independent experiments run in triplicate. Statistical significance of cells co-expressing both receptors compared to cells solely expressing the corresponding receptor is denoted as; ** indicating $p < 0.01$; or *** indicating $p < 0.001$. Statistical significance of cells following OTR or 5-HT treatment compared to the control condition is denoted as; ### indicating $p < 0.001$.

## Downstream signalling changes following the OTR and 5-HTR$_{2A}$ co-expression in cells.

Next, the downstream signalling consequences following co-expression of the OTR and 5-HTR$_{2A}$ were investigated. The OTR and 5-HTR$_{2A}$ are known to mainly signal through the Gαq-mediated pathway, where activation of the Gαq protein leads to generation of the second messenger, D-myoinositol 1,4,5-triphosphate (IP$_3$), causing subsequent intracellular calcium release from the endoplasmic reticulum into the cytoplasm [3,87]. Therefore, we assessed the ligand-mediated changes in intracellular calcium mobilization in HEK293A cells solely expressing the OTR or the 5-HTR$_{2A}$ and

15

cells co-expressing both receptors. The cellular response was detected following the addition of endogenous receptor ligands, OT and 5-HT. The potency of OT ($EC_{50}$ = 0.12 ± 0.01 nM) in cells solely expressing the OTR (HEK293A Lv OTR) and potency of 5-HT ($EC_{50}$ = 12.6 ± 0.7 nM) in cells solely expressing the 5-$HTR_{2A}$ (HEK293A-5-$HTR_{2A}$) were consistent with literature data (Figures 5A and 5B), which confirms the functionality of the receptors expressed in the  heterologous expression system [79,88,89]. Interestingly, the intracellular calcium release following an increasing concentration of OT was significantly reduced in cells co-expressing both the 5-$HTR_{2A}$ and OTR (HEK293A-5-$HTR_{2A}$ Lv OTR) compared to cells expressing only the OTR (Figure 5A). The concentration-response curve of OT was characterized by a significantly lower potency ($EC_{50}$ = 1.0 ± 0.4 nM) and efficacy ($E_{max}$ = 71.1% ± 6.7) in cells co-expressing both receptors compared to cells solely expressing the OTR ($EC_{50}$ = 0.1 ± 0.01 nM, $E_{max}$ = 130.1% ± 15.1) (Figure 5A). Similarly, the concentration-response curve of 5-HT was characterised by a lower potency ($EC_{50}$= 67.5 ± 19.6 nM) but no significant changes in efficacy ($E_{max}$ = 84.3% ± 3.2) in cells co-expressing both receptors compared to cells solely expressing the 5-$HTR_{2A}$ ($EC_{50}$ = 12.6 ± 0.7 nM, $E_{max}$ = 72.0% ± 6.1) (Figure 5B).

The transient release of calcium into the cytosol is also mediated by $IP_3$. Therefore, we evaluated the ligand-mediated changes in the production of this second messenger. The concentrations of OT (10 nM and 1 nM) and 5-HT (100 nM and 10 nM) were chosen based on the calcium assay results (Figures 5A and 5B). As expected, OT-mediated IP-One (inositol monophosphate) accumulation was significantly decreased in cells co-expressing the 5-$HTR_{2A}$/OTR pair compared to cells solely expressing the OTR, depicted as a significant increase in percentage IP-One values of control (Figure 5C). The analogous results were obtained for 5-HT-mediated IP-One accumulation in cells co-expressing both receptors (Figure 5D), validating the observed changes in Gαq-mediated signalling in calcium accumulation assay (Figures 5A and 5B).

In addition, the observed attenuation in ligand-mediated Gαq signalling in cells co-expressing the OTR and 5-$HTR_{2A}$ was shown to be independent of changes in the expression level of both receptors. Flow cytometry analysis of EGFP and tRFP assessed before each experiment showed no changes in the expression level of both receptors between cell lines. The transient transduction with OTR-tRFP did not affect

16

the 5-HTR$_{2A}$-EGFP expression level in cells co-expressing both receptors (HEK293A-5HTR$_{2A}$-EGFP-Lv-OTR-tRFP) compared to non-transduced cells solely expressing the 5-HTR$_{2A}$-EGFP. Similarly, the level of OTR-tRFP expression following transient transduction did not differ in cells co-expressing both receptors compared to cells solely expressing the OTR-tRFP (Figure 4, supplementary data). Control experiments measuring OTR-mediated calcium release between cells stably expressing the OTR-tGFP and cells transiently expressing the OTR-tRFP (following lentiviral transduction) demonstrated no significant differences (Figure 6A, supplementary data). This clearly shows no effect of the gene delivery mode (stable expression versus transient lentiviral transduction) or different fluorescent tags (EGFP or tGFP) on the OTR-mediated G$\alpha$q signalling. Moreover, additional control experiments performed using non-trasfected and non-transduced HEK293A cells as well as HEK293A cells stably expressing tGFP didn't show any unspecific activation of Gq$\alpha$ signalling (Figure 5, supplementary material). Finally, there were no changes in the OTR-mediated calcium response between cells solely expressing the OTR-tGFP and cells co-expressing the OTR-tGFP with OTR-tRFP (following lentiviral transduction), again showing no effect of the lentiviral transduction protocol, nor the OTR overexpression on G$\alpha$q-mediated signalling (Figure 6B, 6C, 6D, supplementary data).

The above results highlight a significant attenuation in the OTR and 5-HTR$_{2A}$-mediated G$\alpha$q signalling, which appears to be dependent on the specific interaction between the two receptors, rather than on changes in their expression level, fluorescent tags or gene delivery mode.
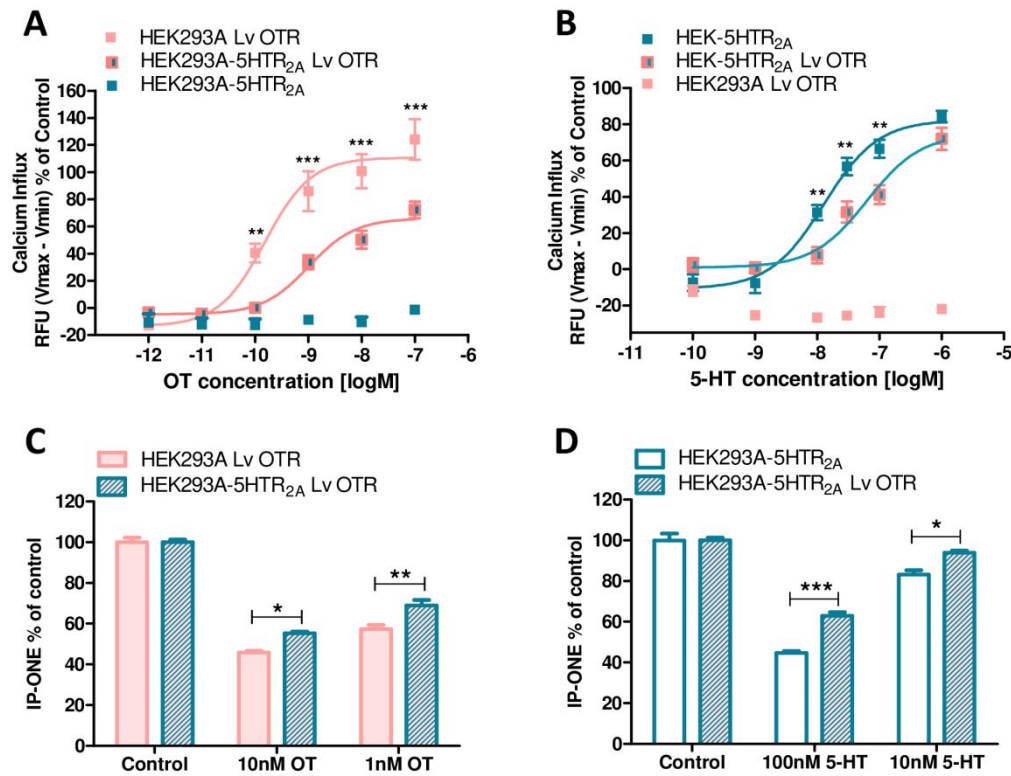
**Figure 5. Co-expression of the OTR and 5-HTR₂ₐ attenuates Gαq-dependent signalling of both receptors.** Intracellular calcium release induced by increasing concentration of OT (A) and 5-HT (B) in HEK293A cells stably expressing the 5-HTR₂ₐ tagged with EGFP, in cells transiently expressing OTR tagged with tRFP, and in cells co-expressing both receptors. Intracellular calcium mobilization is presented as a percentage of maximal calcium response elicited by the control (3% FBS). Graphs represent means ± SEM from at least three independent experiments run in triplicates. IP-One production induced by 10 nM and 1 nM OT (C), and 100 nM and 10 nM 5-HT (D) in HEK293A cells stably expressing 5-HTR₂ₐ tagged with EGFP, in cells transiently expressing OTR tagged with tRFP, and in cells co-expressing both receptors. IP-One production is presented as a percentage of control (100% for non-stimulated cells). Graphs represent means ± SEM from experiments run in triplicate. Statistical significance of cells co-expressing both receptors compared to cells solely expressing one receptor is denoted as * for $p < 0.05$, ** for $p < 0.001$, and *** for $p < 0.001$.

Next, further experiments were performed to investigate if specific antagonists of the OTR and 5-HTR₂ₐ could affect the observed attenuation in the Gαq-dependent downstream signalling pathway. Two antagonists of the OTR (Atosiban and L-371-257) and two antagonists of the 5-HTR₂ₐ (M100907 and Eplivanserin) were used (Figure 6). As expected, both 5-HTR₂ₐ antagonists used in 1 µM concentration were able to inhibit 5-HT-induced calcium mobilization in cells solely expressing the 5-HTR₂ₐ and cells co-expressing both receptors (Figures 6B and 6D). Moreover, the lack of a non-specific interaction between OT and 5-HTR₂ₐ antagonists was demonstrated in cells solely expressing the OTR (Figures 6A and 6C). Although a weak inhibition in OT-induced calcium mobilization after co-administration with M100907 can be

observed, it is not statistically significant (Figure 6A). The lack of non-specific interaction between these two ligands in cells solely expressing the OTR was also confirmed in additional experiments with various concentrations of OT and M100907 (data not shown). Importantly, none of the 5-HTR$_{2A}$ antagonists significantly modulated OT-mediated calcium release in cells co-expressing the OTR and 5-HTR$_{2A}$ (Figures 6A and 6C). These observations for 5-HTR$_{2A}$ antagonists were confirmed following their pre-treatment with cells co-expressing both receptors (Figure 7, supplementary data). Treatment with OTR antagonists (Atosiban and L-371-257) yielded similar results as observed for 5-HTR$_{2A}$ antagonists. Both, Atosiban and L-371-257 used in 1 µM concentration inhibited OT-induced calcium mobilization in cells solely expressing this receptor (Figures 6F and 6H) but did not affect 5-HT-induced calcium signalling in cells co-expressing the OTR and 5-HTR$_{2A}$ (Figures 6E and 6G). Taking together, none of the antagonists used in the experiment were able to modulate the attenuation in Gαq-dependent signalling observed in HEK293A cells co-expressing the OTR-5-HTR$_{2A}$ pair (Figure 5).
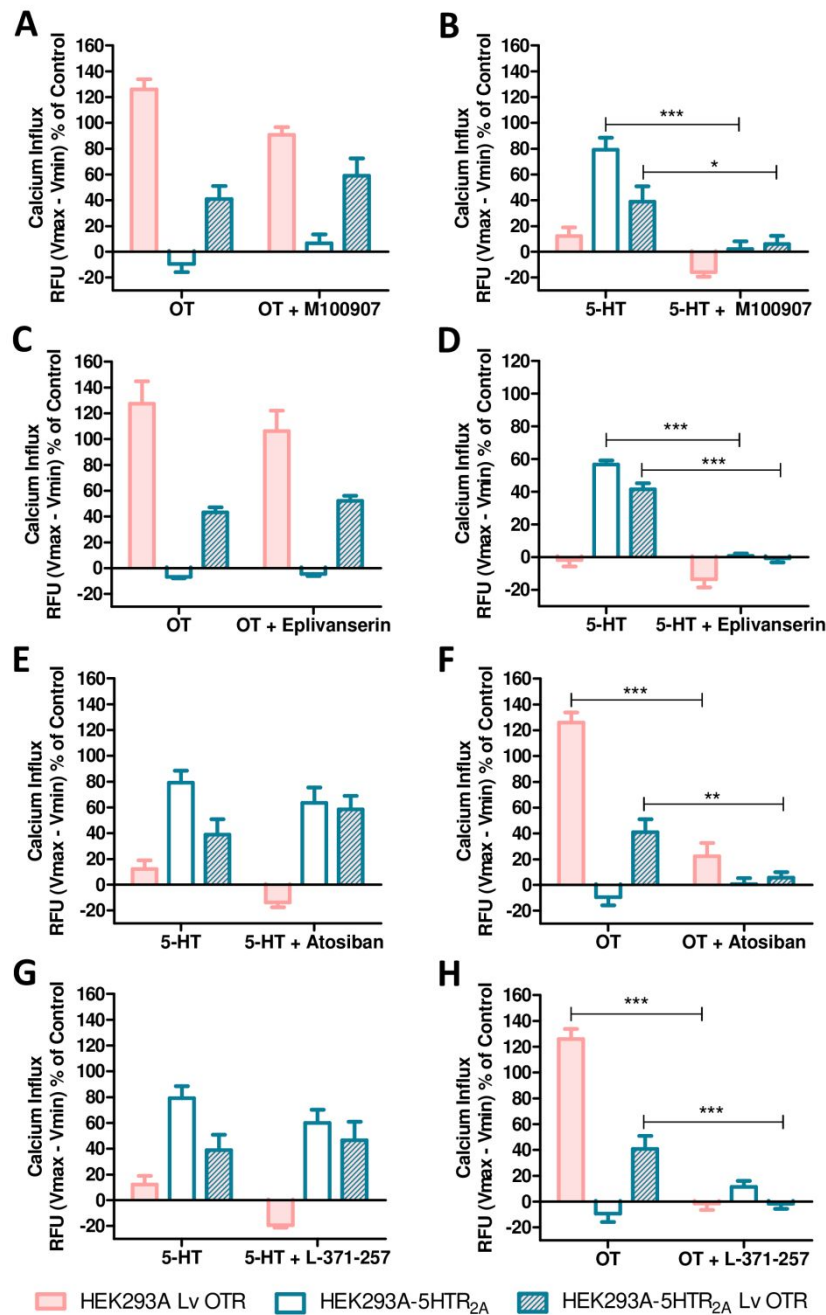
**Figure 6. Pharmacological inhibition of the OTR or 5-HTR$_{2A}$ does not affect the OTR-5-HTR$_{2A}$ heterocomplex specific Gαq-dependent signalling.** Intracellular calcium release in cells solely expressing OTR, cells solely expressing 5-HTR$_{2A}$, and cells co-expressing both receptors induced by 10 nM OT alone and in the presence of 1 µM 5-HTR$_{2A}$ antagonists; M100907 (A) and Eplivanserin (C), as well as 1 µM OTR antagonists; Atosiban (F) and L-371-257 (H). Intracellular calcium release induced by 100 nM 5-HT alone and in the presence of 1 µM OTR antagonists; Atosiban (E) and L-371-257 (G), as well as 5-HTR$_{2A}$ antagonists; M100907 (B) and Eplivanserin (D). All graphs represent means ± SEM from at least two independent experiments run in triplicates, demonstrated as percentage of maximum calcium response (3% FBS). Statistical significance of cells co-expressing both receptors compared to cells solely expressing corresponding receptor is denoted as * for $p < 0.05$, ** for $p < 0.001$, and *** for $p < 0.001$.

The effect of the 5-HTR$_{2A}$ on OTR-dependent Gαq signalling induced by OT is more pronounced in our in vitro model compared to the effect of the OTR on 5-HTR$_{2A}$. Thus, to further investigate pronounced alteration in OTR-mediated Gαq signalling, cells with the co-expression of the OTR and 5-HTR$_{2A}$ were treated with different concentrations of two synthetic OTR agonists; carbetocin and WAY267464 [90,91]. Similar to what we observed for OT, the intracellular calcium release induced by increasing concentrations of carbetocin and WAY267464 was significantly reduced in cells co-expressing the 5-HTR$_{2A}$ and OTR compared to cells solely expressing the OTR (Figure 7). The potency and efficacy of carbetocin was significantly lower (EC$_{50}$= 9.4 ± 2.5 nM, E$_{max}$ = 21.9% ± 4.1) in cells co-expressing both receptors compared to cells solely expressing the OTR (EC$_{50}$ = 0.5 ± 0.3 nM, E$_{max}$ = 86.0% ± 11.0) (Figure 7A). Intracellular calcium response induced by increasing concentrations of WAY267464 was completely abolished in cells co-expressing the OTR and 5-HTR$_{2A}$ (EC$_{50}$= nc, E$_{max}$ = 2.7% ± 1.5) compared to cells solely expressing the OTR (EC$_{50}$= 11.6 nM, E$_{max}$ = 61.2% ± 1.2) (Figure 7B). Nevertheless, pre-treatment of cells with 5-HTR$_{2A}$ antagonist (eplivanserin) did not affect carbetocin (Figure 7C) nor WAY267464 (Figure 7D) induced calcium response in cells co-expressing both receptors. In the same experimental setup, eplivanserin was able to inhibit 5-HT-mediated intracellular calcium accumulation in cells solely expressing the 5-HTR$_{2A}$ confirming compound specificity (data not shown).
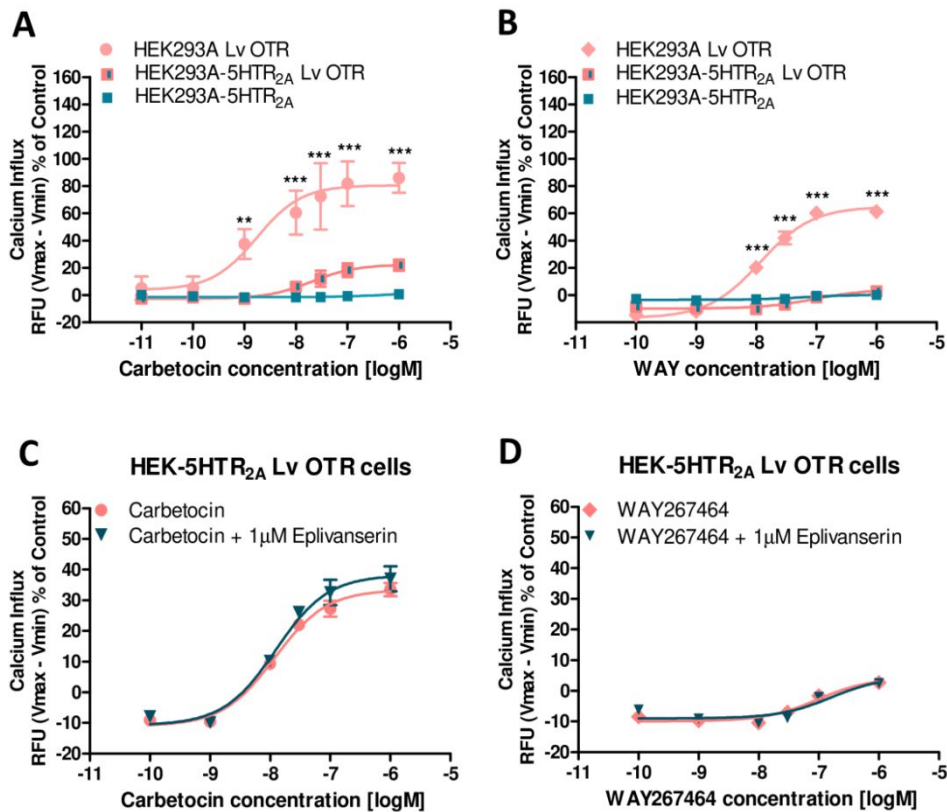
**Figure 7. Synthetic OTR ligand-mediated attenuation of Gαq-dependent signalling in cells co-expressing the OTR and 5-HTR$_{2A}$.** Intracellular calcium release induced by increasing concentration of Carbetocin (A) and WAY265464 (B) in cells expressing OTR, in cells expressing 5-HTR$_{2A}$, and in cells co-expressing both receptors. Graphs present mean ± SEM from et least two independent experiments run in triplicates. Statistical significance of cells co-expressing both receptors compared to cells solely expressing corresponding receptor is denoted as ** for $p < 0.001$, and *** for $p < 0.001$. Intracellular calcium release induced by increasing concentration of Carbetocin (C) and WAY (D) in the presence of 5-HTR$_{2A}$ antagonist; Eplivanserin in cells co-expressing both receptors. Graphs present mean ± SEM from an experiment run in triplicate. Results are demonstrated as a percentage of maximum calcium response (3% FBS).

The results clearly show that one receptor induces highly reproducible functional attenuation in partner receptor signalling. A significant decrease in 5-HTR$_{2A}$ dependent signalling has been demonstrated upon co-expression with the OTR. The attenuated OTR-mediated signalling is even more evident compared to 5-HTR$_{2A}$-mediated signalling changes. These interesting observations may be related to conformational rearrangements of one protomer resulting in trans-inhibition of another after agonist binding. Moreover, the lower potency and efficacy of OTR agonists are completely in line with the increasing attenuation of the receptor downstream signalling (Figures 5A, 7A and 7B). This may suggest that the potency of receptor ligands to activate Gαq signalling is lower for the OTR-5-HTR$_{2A}$ heteromer complexes than for the corresponding receptor homodimers. Interestingly, current findings are in line with

antagonistic interactions previously observed between the 5-HTR$_{2A}$ and mGluR2 which have been established *in vitro* in heterologous expression models and across multiple *ex vivo* and *in vivo* studies [57,60]. The formation of 5-HTR$_{2A}$ heteromeric complexes with the D2R has also been demonstrated to result in D2R-mediated Gαi signalling attenuation [48]. In contrast, concomitant activation of the D2R was shown to increase the 5-HTR$_{2A}$-mediated Gαq signalling. Thus, the existence of a 5-HTR$_{2A}$-mediated D2R trans-inhibition mechanism was suggested. Considering the above, the 5-HTR$_{2A}$ in heteroreceptor complexes with other GPCRs has a tendency to inhibit downstream signalling of the partner receptor. This further supports 5-HTR$_{2A}$-mediated inhibition of the OTR-dependent signalling observed in the current study. Interestingly, previous findings also demonstrated changes in downstream OTR signalling following the formation of OTR heteroreceptor complexes with other GPCRs [50,53]. In the case of OTR-D$_2$R heterodimers both the Gq/11 and the MAPK pathways activation have been increased [53]. By simple analogy we could hypothesize that co-expression of the OTR and 5-HTR$_{2A}$ in HEK293A cells may also affect other signalling pathways including MAPK cascade. However, based on the broader literature and also our own experience specific heteromers are often able to only affect a single G-protein-dependent signalling pathway [66]. Evidence also suggests that GPCR heteromers can activate signalling cascades which are not activated by the individual protomers not in the complex [92]. Additionally, different ligands can differently alter signalling pathways mediated by the formation of heteroreceptor complexes (biased signalling) [54,93]. Thus, further studies investigating the full spectrum of downstream signalling pathways following modulation by different receptors ligands and their specific effects on the OTR-5-HTR$_{2A}$ heteroreceptor are now warranted.

Taking together the above, previously described heteroreceptor complexes of the 5-HTR$_{2A}$ with mGlu2 and D2R, as well as formation of heteromers between the OTR and D2R, were shown to produce allosteric receptor-receptor interactions between the two protomers [48,53,60]. Current results provide evidence that the formation of stable OTR-5-HTR$_{2A}$ heterocomplexes leads to bidirectional antagonistic receptor-receptor interactions with greater 5-HTR$_{2A}$ dominance. However, unlike previous studies, the antagonists of both OTR and 5-HTR$_{2A}$ did not affect the specific signalling driven by OTR-5-HTR$_{2A}$ heterocomplexes. Moreover, there was no synergistic nor additive effect in Gqα signalling when cell co-expressing both receptors were co-treated with their respective endogenous ligands, OT and 5-HT (Figure 8, supplementary data).

Thus, one of the possible mechanisms of this specific receptor-receptor interaction is the physical binding between the two protomers and subsequent conformational changes without a steric hinderance of the binding pockets.

**CONCLUSION**

GPCRs comprise the largest family of cell surface receptors, which are major signalling mediators for many hormones and neurotransmitters involved in diverse physiological functions ranging from glucose metabolism to neurotransmission. GPCRs were originally thought to function as monomers. However, oligomerization of these receptors has now become accepted as a fundamental process in GPCR signalling. Oligomerization of specific GPCR protomers is characterized by an increased receptor signalling diversity and exhibits unique functional and pharmacological properties adding a new dimension to GPCR pharmacology. Since mechanisms that lead to diverse brain pathologies such as social and cognition related disorders involve GPCR signalling, the distinct pharmacological profiles of GPCR assemblies may serve as novel mechanisms, important for the development of more specific pharmacological strategies to modulate cell response and regulate many physiological processes.

This study shows compelling evidence for a functionally relevant formation of a novel heteroreceptor complex between the OTR and 5-HTR$_{2A}$. Both receptors have been shown to physically interact in living mammalian cells co-expressing both receptors (Figure 1). Confocal microscopy demonstrated that this specific interaction seems to appear at the cell membrane as well as intracellularly (Figure 2). Alterations in the trafficking of both receptors within the cell and their significant intracellular presence in basal conditions (Figure 4) are in line with the colocalized expression and strongly suggests changes in OTR and 5-HTR$_{2A}$ maturation and trafficking to the cell membrane. However, this phenomenon may also be a consequence of increased coupling to β-arrestin and subsequently higher basal activity of the two receptors. In any case both hypothesis support a physical interaction between the OTR and 5-HTR$_{2A}$ within the cell. Noteworthy, a significant attenuation was demonstrated primarily in OTR but also in 5-HTR$_{2A}$-mediated Gαq-dependent signalling (Figure 5 and 7) indicating a functional relevant consequence of OTR/5-HTR$_{2A}$ interaction. In conclusion, the current study provides evidence that the OTR-5HTR$_{2A}$ heterocomplex formation leads to bidirectional antagonistic receptor-receptor interactions *in vitro* in

the heterologous system. As the antagonists of both receptors did not affect OTR-5HTR$_{2A}$ heterocomplex specific signalling (Figure 6), it is likely that the physical binding between the two protomers serves as a mechanism for this specific receptor-receptor crosstalk.

Moreover, the formation of OTR-5HTR$_{2A}$ heteroreceptor complexes were demonstrated *ex vivo* in rat brain sections using *in situ* PLA technique (Figure 3). OTR-5HTR$_{2A}$ heteroreceptor complexes were observed in the pyramidal cell layer of CA2-CA3 regions of the hippocampus, the layers II and III of the cingulate cortex and in a number of nerve cell bodies of the nucleus accumbens shell and core. The proximal dendrites of these nerve cells had a low number of PLA clusters located close to them. This specific distribution pattern may indicate the potential role of OTR-5-HTR$_{2A}$ heteroreceptor complexes in distinct cortical and subcortical limbic regions. The formation of these receptor complexes may therefore have special role in distinct limbic circuits of relevance for social salience and memory, bearing in mind the importance of OTR in social interactions.

The existence of novel functional OTR-5HTR$_{2A}$ heteroreceptor complexes constitutes one of the possible mechanisms for intriguing interactions between the OT and 5-HT neurotransmitter systems. It also provides potential novel therapeutic strategies in the treatment of social and cognition-related diseases. Further *in vivo* studies exploring the physiological and behavioural nature of the specific interactions observed between the OTR and 5-HTR$_{2A}$ in limbic regions are now warranted.

## METHODS

### Receptors ligands.

Oxytocin (OT) (#O3251), carbetocin (#SML0748), 5-hydroxytryptamine (5-HT) (#H9523), atosiban (#A3480), and M100907 (#M3324) were purchased from Sigma-Aldrich (Wicklow, Ireland). L-371-257 (#2410), WAY267464 (#3933) and eplivanserin hemifumarate (#4958) were purchased from Tocris Bioscience (Ellisville, MO). A 3 mM stocks of compounds were prepared in $H_2O$ (oxytocin, carbetocin, 5-HT, atosiban, M100907, WAY267464, eplivanserin hemifumarate) or in DMSO (L-371-257). All compound stocks were further diluted to the required concentrations in the proper assay buffer.

### Cell culture and stable transfection.

Plasmid containing the canonical sequence (transcript variant 1) of the human serotonin 2A receptor (5-HTR$_{2A}$) (NM_000621) was supplied from University of Missouri–Rolla (#HTR02ATN00). The coding sequence of the receptor lacking its stop codon was amplified using forward 5'-AGCTCGAGACCATGGATATTCTTTGTGAAGAAAATAC-3' and reverse 5'-GAGAGGATCCCACACACAGCTCACC-3' primers containing XhoI and BamHI restriction sites, respectively. The amiplified sequence was then subcloned into the multicloning site of the pCMV-EGFP-N1 vector (Clontech #6085-1) to obtain the 5-HTR$_{2A}$ C-terminally tagged with EGFP. The obtained plasmid construct; pCMV-5-HTR2A-EGFP-N1 was verified by restriction analysis, sequencing and then used for stable transfection of Human Embryonic Kidney (HEK293A) cells.

HEK293A cells (Invitrogen, Carlsbad, CA) were cultured in high glucose Dulbecco's modified Eagle's medium (DMEM, #D5796; Sigma-Aldrich, Wicklow, Ireland) supplemented with 10% heat inactivated Fetal Bovine Serum (FBS) (#F7524; Sigma-Aldrich) and 1% Non-Essential Amino Acids (NEAA) (#11140035; Gibco Life Technologies, Gaithersburg, MD). Cells were maintained at 37°C in a humidified atmosphere with 5% $CO_2$. HEK293A cells were transfected with the plasmid containing human 5-HTR$_{2A}$ sequence fused with EGFP in the presence of Lipofectamine LTX Plus reagent, according to the manufacturer's instructions (#15338100; Invitrogen). 48 h after transfection, the cell media was changed for DMEM supplemented with 500 ng/μl G-418 (#345812; Calbiochem), allowing for the

selection of cells with stably integrated pCMV-5-HTR2A-EGFP-N1 plasmid. The cells with the highest expression of the receptor were selected using flow-assisted cell sorting (FACSAriaII, BD Biosciences), followed by clonal expansion in 96-well plates. Expression level of 5-HTR$_{2A}$ in generated monoclonal cell line was routinely monitored using an epifluorescence microscope (Olympus IX70) and a flow cytometer (FACSCalibur, BD Biosciences).

**Lentiviral transfection and transduction.**

The coding sequences of the human oxytocin receptor (OTR) was subcloned into the multicloning site of the HIV-based, replication deficient, lentiviral expression vector; pHR-SIN-BX-tRFP. The construct containing the canonical sequence of the human OTR (NM_000916.3), C-terminally tagged with red fluorescent protein (tRFP) was generated by inserting the coding sequence of the receptor lacking its stop codon from pCMV6-AC-OXTR-GFP plasmid (#RG211797; OriGene, Rockville, MD) into the target vector (pHR-SIN-BX-tRFP) with the use of BamHI and XhoI restriction enzymes. The obtained pHR-SIN-BX-OXTR-tRFP plasmid construct was validated by restriction analysis and DNA sequencing. HEK293A cells were then transiently transduced with the obtained lentiviral expression vector using a second generation packaging, gene delivery, viral vector production system, previously described by our group [64]. Briefly, HIV-based lentiviral particles containing the OTR sequence were produced using HEK293T-17 cells, by transient co-transfection of the expression construct; pHR-SIN-BX- OXTR -tRFP, the packaging construct; pCMV ΔR8.91, and the envelope construct; pMD.G-VSV-G. Following this, HEK293A cells were transiently transduced with the OTR-tRFP expressing lentiviral particles diluted in transduction media, consisting of DMEM with 2% FBS, 1% NEAA, and 8 µg/ml polybrene (#H9268; Sigma). The efficiency of transduction was monitored with the use of an epifluorescence microscope (Olympus IX70) and a flow cytometer (FACSCalibur, BD Biosciences) before each experiment.

**Flow Cytometry Fluorescence Resonance Energy Transfer (fcFRET).**

HEK293A cells stably expressing 5-HTR$_{2A}$ tagged with EGFP were transiently transduced with lentiviral OTR sequence tagged with tRFP. Following transduction, cells were washed with PBS and mechanically removed from the wells. Cell suspension was then centrifuged for 4 min at 200 x g, at room temperature. The pellet

of cells was re-suspended in 400 µl of 2 nM EDTA (#E5134; Sigma) in PBS. Prior to analysis cells were passed through a 100 µm nylon mesh cell strainer (#10199-658; VWR) and collected in a 5 ml round bottom polystyrene tubes (#352054; Corning). The fcFRET analysis was performed on a FACS AriaII cytometer (BD Biosciences) according to the protocol optimized in our group (Chruścicka et al., 2018; Schellekens et al., 2015). Briefly, EGFP was excited at 488 nm from blue laser and detected with a 525/50 nm bandpass filter, whereas tRFP was excited at 561 nm from yellow/green laser and detected with a 610/20 nm bandpass filter. FRET signal between EGFP and tRFP was measured by excitation at 488 nm from blue laser and detection with a 610/20 nm bandpass filter located on the same laser. For the proper separation of EGFP fluorescence and FRET emission from blue laser, a 505 Long Pass (LP) dichroic mirror (DM) was used. Wild-type HEK293A cells were used for initial instrument setup and to differentiate cells based on their size and granulation, according to forward and side scattering plot (FSC/SSC), which allowed to eliminate doublets, dead cells, and debris from further analysis. In the next step, cells expressing donor or acceptor construct only were used to fine tune PMT settings and to perform the proper compensation for spectral bleed through, in particular for EGFP emission in the tRFP-fcFRET detector. In addition, cells co-expressing the donor construct (GPCR-EGFP) with the control acceptor construct (control-tRFP; plasmid with the sequence of tRFP without the receptor) were used to further control unspecific fcFRET signal coming from the cross-excitation. The same number of cells ($10^4$) was recorded for each sample. Data was analysed using BD FACSDiva (BD Biosciences).

**Colocalization with the use of confocal microscope.**

HEK293A stably expressing 5-HTR$_{2A}$-EGFP were transiently transduced to co-express OTR-tRFP. Following transduction, cells were passaged and seeded on poly-L-lysine-coated (#P4707; Sigma) borosilicate glass slides (#631-0150; VWR International) at the density of 5 x $10^5$ cells per well of 24-well plate, followed by 24 h incubation in the standard culture conditions. Co-localization of the receptors was assessed in living cells using laser scanning confocal fluorescent microscope (FV 1000 Confocal System; Olympus). Pictures were taken with 63 x objective lens using Olympus fluoview FV3000 software. Co-localization between 5-HTR$_{2A}$-EGFP and OTR-RFP was analysed by overlay with the use of ImageJ software (US National Institutes of Health).

### Receptors trafficking assay.

The trafficking of receptors was analysed by monitoring the fluorescent proteins translocation away from the cellular membrane into vesicles within the cytosol. HEK293A cells stably expressing the 5-HTR$_{2A}$-EGFP and transduced with lentiviral OTR-tRFP, were seeded on 24-well plates (#83.3922.005; Sarstedt) at the density of 5 x 10$^4$ cells/well. Cells were then incubated for 48 h at standard culture conditions. 24 h before experiment, media was replaced with serum-free DMEM containing 1% NEAA. To investigate ligand-mediated changes in receptors trafficking, cells were incubated with different concentrations of 5-HTR$_{2A}$ or OTR endogenous agonists for 30 minutes at 37$^o$C. After the treatment, cells were fixed in 4% paraformaldehyde (PFA) for 20 min and washed two times in PBS. Ligand mediated internalization of the receptors was assessed using inverted fluorescence microscope (IX71; Olympus). Fluorescent images were acquired with 20 x objective lens using Olympus cell R software. Results demonstrated in the manuscript represent average from 3 independent experiments each performed in duplicates (two wells for each condition in each experiment). Within each well, three images were captured. For each image 6 cells were quantitatively analysed by two independent researchers. Quantification of the receptors trafficking was assessed by calculating the ratio between subcellular and membrane fluorescent intensity after excluding background fluorescence, with the use of Java image processing program (ImageJ, US National Institutes of Health). The obtained results were depicted using GraphPad Prism software (PRISM 5.0; GraphPAD Software Inc., San Diego, CA).

### Animals

All experiments were performed using male Sprague-Dawley rats (SD) (Scanbur, Sweden). The animals were group-housed under standard laboratory conditions (20–22°C, 50–60% humidity). Food and water available *ad libitum*. The rats were 3–4 months of age at the time of experiments. All studies involving animals were performed in accordance with the Stockholm North Committee on Ethics of Animal Experimentation, the Swedish National Board for Laboratory Animal and European Communities Council Directive (Cons 123/2006/3) guidelines for accommodation and care of Laboratory Animals.

### *In situ* proximity ligation assay (*in situ* PLA)

To study the OTR-5HTR$_{2A}$ heteroreceptor complexes the *in situ* proximity ligation assay (*in situ* PLA) was performed as described previously [94]. Adult age-matched male Sprague–Dawley rats (n=4) were anaesthetized and perfused intracardially with 4% (wt/vol) formalin in saline. Brains were removed, post-fixed by immersion overnight in 4% formalin in PBS and coronal sections (30 μm) were cut on a cryostat and processed for free-floating *in situ* PLA. Free-floating formalin fixed brain sections (storage at −20°C in Hoffman solution) at Bregma level (-3.6 mm and 1.2 mm) were washed four times with PBS and quenched with 10 mM Glycine buffer for 20 min at room temperature. Then, after three PBS washes, were permeabilized with a permeabilization buffer (10% FBS and 0.5% Triton X-100 or Tween 20 in Tris buffer saline (TBS), pH 7.4) for 30 min at room temperature. Again the sections were washed twice, 5 min each, with PBS at room temperature and incubated with the blocking buffer (0.2% BSA in PBS) for 30 min at room temperature. The brain sections were then incubated with the primary antibodies diluted in a suitable concentration in the blocking solution for 1-2 h at 37°C or at 4°C overnight. The day after, the sections were washed twice, and the proximity probe mixture was applied to the sample and incubated for 1 h at 37°C in a humidity chamber. The unbound proximity probes were removed by washing the slides twice, 5 min each time, with blocking solution at room temperature under gentle agitation and the sections were incubated with the hybridization-ligation solution (BSA (250 g/ml), T4 DNA ligase (final concentration of 0.05 U/μl), 0.05% Tween-20, 250 mM NaCl, 1 mM ATP and the circularization or connector oligonucleotides (125-250 nM)) and incubated in a humidity chamber at 37°C for 30 min. The excess of connector oligonucleotides was removed by washing twice, for 5 min each, with the washing buffer A (Sigma-Aldrich, Duolink Buffer A (8.8 g NaCl, 1.2 g Tris Base, 0.5 ml Tween 20 dissolved in 800 ml high purity water, pH to 7.4) at room temperature under gentle agitation and the rolling circle amplification mixture was added to the slices and incubated in a humidity chamber at 37°C for 100 min. Then, the sections were incubated with the detection solution in a humidity chamber at 37°C for 30 min. In a last step, the sections were washed twice in the dark, for 10 min each, with the washing buffer B (Sigma-Aldrich, Duolink Buffer B (5.84 g NaCl, 4.24 g Tris Base, 26.0 g Tris-HCl. Dissolved in 500 ml high purity water, pH 7.5) at room temperature under gentle agitation. The free-floating sections were put on a microscope slide and a drop of appropriate mounting medium (e.g., VectaShield or Dako) was applied. The cover slip was placed on the section and sealed with nail

polish. The sections were protected against light and stored for several days at −20°C before confocal microscope analysis. The in situ PLA experiments were performed using the following primary antibodies: rabbit monoclonal anti-5-HTR$_{2A}$ (#SAB4301791, 1 µg/ml; Sigma-Aldrich, Stockholm, Sweden) and goat polyclonal anti-oxytocin receptor (#ab87312, 5µg/ml; Abcam, Stockholm, Sweden). As a neuronal marker the Neuro-ChromTM Pan neuronal marker antibody-Alexa488 conjugated (#ABN2300A4, Merck/Sigma-Aldrich) was used. The PLA signal was visualized and quantified by using a Leica TCS-SL confocal microscope (Leica, USA) and the Duolink Image Tool software. A range of positive and negative controls have been used to guarantee the specificity of the PLA signal. The negative control consists in the suppression of the species-specific primary antibody corresponding to the 5-HTR$_{2A}$ in the presence of the two PLA probes. As a positive control of the PLA assay, a parallel analysis of the 5-HTR$_{1A}$-5HTR$_{2A}$ isoreceptor complexes and the D$_2$R-OTR heteroreceptor complexes have been performed. Detailed quality control analysis for the 5HTR$_{2A}$ and for the OTR antibodies have been reported previously [49,63]. Furthermore, both anti-5HTR$_{2A}$ and anti-OTR antibodies were previously validated in our team in terms of their quality (in Western blot in collaboration with Human Atlas project and in HEK293 cells with and without expression of each receptor subtype using confocal analysis). Antibodies were used under optimal conditions, taking into consideration parameters, such as; concentration, targeted epitopes, fixation conditions, and antigen-retrieval [94].

**Intracellular calcium mobilization assay.**

Receptor-mediated changes in intracellular calcium (Ca$^{2+}$) were monitored with the use of automatic fluorescent reader, FLIPR Tetra® (Molecular Devices, LLC Sunnyvale, CA) as previously described [54,95]. HEK293A cells with the expression of the receptors under investigation were seeded in black 96-well microtiter plates at a density of 3.0 - 4.0 x 10$^4$ cells/well and incubated overnight in standard culture conditions. 24 h prior to the experiment growth media was replaced with serum-free DMEM containing 1% NEAA. At the day of experiment cells were incubated for 90 min with 80 µl of the Ca5 dye diluted in assay buffer containing 1 x Hank's Balanced Salt Solution; HBSS (#14065049; Gibco Life Technologies, Gaithersburg, MD) and 20 mM HEPES (#H0887; Sigma-Aldrich) in the concentration recommended by the manufacturer's protocol (#R8186; Molecular Devices). The addition of receptor ligands

(40 μl/well) was performed with the use of automatic pipettor of the FLIPR Tetra®High-Throughput Cellular Screening System. To investigate the effect of receptor antagonists, compounds were co-administered together with agonist or pre-incubated for 90 min with the Ca5 dye. Fluorescent readings were taken for a total of 120 seconds with excitation wavelength of 485 nm and emission wavelength of 525 nm. The relative increase in intracellular calcium [$Ca^{2+}$] was calculated as the difference between the maximum and baseline fluorescence, and demonstrated as percentage relative fluorescent units (RFU) normalized to maximum response (100% signal) obtained for 3% FBS. Background fluorescence was recorded for non-stimulated cells and subtracted from RFU. Data were analysed using GraphPad Prism software (PRISM 5.0; GraphPAD Software Inc., San Diego, CA). The concentration-response curves of receptor ligands were generated using the nonlinear regression. The curves were fitted to a 3-parametric logistic equation, allowing for the determination of $EC_{50}$ values.

**HTRF based IP-One accumulation assay.**

The detection of IP-One (inositol monophosphate) was performed in HEK293A cells expressing receptors under investigation, with the use of a homogeneous time-resolved fluorescence (HTRF) IP-One assay (#62IPAPEB; Cisbio, Codolet, France). The assay was performed according to the manual's instruction provided by Cisbio with minor modifications. Briefly, 24 h before experiment growth media was replaced with serum-free DMEM containing 1% NEAA. Directly before the experiment cells were scraped and centrifuged for 3 min at 200 x g. The cell pellet was then suspended in assay buffer (146 mM NaCl, 1 mM $CaCl_2$, 10mM HEPES, 0.5 mM $MgCl_2$, 4.2 mM KCl, 5.5 mM glucose) containing 50 mM LiCl to inhibit degradation of IP-One. For the stimulation step, 35 μL of cell suspension was pipetted to a flat bottom 96-well plate at the density of 3 x $10^5$/well (#655075; Greiner Bio-One International) containing the appropriate concentration of compounds. Cells were incubated with compounds for 1 h at 37 °C. Following this step, 15 μL of IP1-d2 conjugate and 15 μL of anti-IP1 cryptate conjugate diluted in lysis buffer were added and incubated for 1 h in room temperature. After 1 h of incubation, the fluorescence at 620 nm and 665 nm was read with the use of FlexStation instrument (Molecular Devices, LLC Sunnyvale, CA) and the readout setup recommended by the company (Cisbio, Codolet, France). The results were calculated as the 665-nm/620-nm ratio multiplied by $10^4$ and depicted as percentage

of relative fluorescent units (RFU) normalized to maximum response (100% signal) obtained for non-stimulated cells. The specific signal is inversely proportional to the concentration of endogenous IP-One in the sample. Data were analysed using GraphPad Prism software (PRISM 5.0; GraphPAD Software Inc., San Diego, CA).

**Statistical analysis.**

Data were analyzed using GraphPad Prism software (PRISM 5.0; GraphPAD Software Inc., San Diego, CA). The concentration-response curves of receptors ligands were generated using the nonlinear regression. The curves were fitted to a 3-parametric logistic equation, allowing for the determination of $EC_{50}$ and $E_{max}$ values. Statistical comparison of the concentration-response curves parameters ($EC_{50}$ and $E_{max}$) between cells co-expressing both receptors and cells solely expressing the corresponding receptor, were performed using the Student's test. Moreover, statistical comparison of each compound concentration used in calcium mobilization, IP-One accumulation, and ligand-mediated internalization assays between cells expressing the OTR, $5HTR_{2A}$ and cells co-expressing both receptors was performed using Two-way ANOVA with Bonferroni's multiple comparison tests. Statistical analysis of fcFRET was performed using One-way ANOVA with Bolferroni's multiple comparison tests. Statistical analysis of In situ PLA was performed using One-way ANOVA followed by Tukey post-test. All data are presented as Mean ± SEM. The differences between groups were considered significant for $p < 0.05$. The number of independent experiments performed is provided in figure legends.

**ASSOCIATED CONTENT**

**Supporting information**

Graphs presenting the results of additional control experiments: Figure S1. fcFRET signal between the OTR-tGFP and the OTR-tRFP; Figure S2. fcFRET signal between the tGFP and the tRFP; Figure S3. Confocal images presenting the expression pattern of the OTR-tRFP in HEK293A. Figure S4. Flow cytometry analysis of EGFP and tRFP in cells co-expressing receptors under investigation; Figure S5. The effect of OTR ligands on intracellular calcium release in HEK293A and HEK293A-tGFP cells. Figure S6. The effect of transduction procedure and fluorescent tags on Gαq-dependent signalling; Figure S7. The effect of $5$-$HTR_{2A}$ antagonists on the OTR-mediated Gαq signalling; Figure S8. The effect of OT and 5-HT co-treatment on Gαq-mediated signalling in cells co-expressing $5$-$HTR_{2A}$ and OTR.

## AUTHOR INFORMATION

### Corresponding author

E-mail H.Schellekens@ucc.ie. Tel +353 (0)21 420 54 29

### Author Contributions

B.Ch. designed all in vitro experiments, performed experiments that lead to Figures 1, 2, 5, 6, 7, analysed all in vitro results and wrote the manuscript. S.W.F. performed transduction of cells for all in vitro experiments, performed and analysed experiments that lead to Figure 4. D.B.E. designed, performed and analysed all ex vivo data. C.D. served technician assistant in maintenance of cells, preparation of plasmid constructs and calcium assay experiments. S.P. served as technician support in designing and performing of fcFRET experiments. J.F.C., T.G.D., K.N. and K.F. supervised the work and critically read the manuscript. H.S. was involved in the conception of all experiments, supervised the work and edited the manuscript.

### Notes

The authors declare no conflict of interest.

**REFERENCES**

1. Vigneaud V, RESSLER C, TRIPPETT S. The sequence of amino acids in oxytocin, with a proposal for the structure of oxytocin. *J. Biol. Chem.* 1953;205(2):949-57. Available at: http://www.ncbi.nlm.nih.gov/pubmed/13129273.

2. Graf GC. Ejection of milk in relation to levels of oxytocin injected intramuscularly. *J. Dairy Sci.* 1969;52(7):1003-7. doi:10.3168/jds.S0022-0302(69)86684-1.

3. Gimpl G, Fahrenholz F. The oxytocin receptor system: structure, function and regulation. *Physiol. Revs.* 2001;81(2):630-683.

4. Young WS, Shepard E, Amico J, et al. Deficiency in mouse oxytocin prevents milk ejection, but not fertility or parturition. *J. Neuroendocrinol.* 1996;8(11):847-53. Available at: http://www.ncbi.nlm.nih.gov/pubmed/8933362.

5. Arrowsmith S, Wray S. Oxytocin: Its mechanism of action and receptor signalling in the myometrium. *J. Neuroendocrinol.* 2014;26(6):356-369. doi:10.1111/jne.12154.

6. Zingg HH, Laporte SA. The oxytocin receptor. *Trends Endocrinol. Metab.* 2003;14(5):222-227. doi:10.1016/S1043-2760(03)00080-8.

7. Kimura T, Tanizawa O, Mori K, Brownstein MJ, Okayama H. Structure and expression of a human oxytocin receptor. *Nature* 1992;356(6369):526-9. doi:10.1038/356526a0.

8. Welch MG, Margolis KG, Li Z, Gershon MD. Oxytocin regulates gastrointestinal motility, inflammation, macromolecular permeability, and mucosal maintenance in mice. *AJP Gastrointest. Liver Physiol.* 2014;307(8):G848-G862. doi:10.1152/ajpgi.00176.2014.

9. Li T, Wang P, Wang SC, Wang Y-F. Approaches Mediating Oxytocin Regulation of the Immune System. *Front. Immunol.* 2016;7:693. doi:10.3389/fimmu.2016.00693.

10. Imanieh MH, Bagheri F, Alizadeh AM, Ashkani-Esfahani S. Oxytocin has therapeutic effects on cancer, a hypothesis. *Eur. J. Pharmacol.* 2014;741:112-23. doi:10.1016/j.ejphar.2014.07.053.

11. Lee HJ, Macbeth AH, Pagani JH, Scott Young W. Oxytocin: The great facilitator of life. *Prog. Neurobiol.* 2009;88(2):127-151. doi:10.1016/j.pneurobio.2009.04.001.

12. Mustoe A, Taylor JH, French JA. Oxytocin Structure and Function in New World Monkeys: From Pharmacology to Behavior. *Integr. Zool.* 2018. doi:10.1111/1749-4877.12318.

13. De Dreu CKW. Oxytocin modulates cooperation within and competition between groups: an integrative review and research agenda. *Horm. Behav.* 2012;61(3):419-28. doi:10.1016/j.yhbeh.2011.12.009.

14. Meyer-Lindenberg A, Domes G, Kirsch P, Heinrichs M. Oxytocin and vasopressin in the human brain: Social neuropeptides for translational

medicine. *Nat. Rev. Neurosci.* 2011;12(9):524-538. doi:10.1038/nrn3044.

15.  Borland JM, Rilling JK, Frantz KJ, Albers HE. Sex-dependent regulation of social reward by oxytocin: an inverted U hypothesis. *Neuropsychopharmacology* 2018;(April):1-14. doi:10.1038/s41386-018-0129-2.

16.  Neumann ID, Slattery DA. Oxytocin in General Anxiety and Social Fear: A Translational Approach. *Biol. Psychiatry* 2016;79(3):213-221. doi:10.1016/j.biopsych.2015.06.004.

17.  Strauss GP, Chapman HC, Keller WR, et al. Endogenous oxytocin levels are associated with impaired social cognition and neurocognition in schizophrenia. *J. Psychiatr. Res.* 2019;112:38-43. doi:10.1016/j.jpsychires.2019.02.017.

18.  Husarova VM, Lakatosova S, Pivovarciova A, et al. Plasma Oxytocin in Children with Autism and Its Correlations with Behavioral Parameters in Children and Parents. *Psychiatry Investig.* 2016;13(2):174-83. doi:10.4306/pi.2016.13.2.174.

19.  Sobota R, Mihara T, Forrest A, Featherstone RE, Siegel SJ. Oxytocin reduces amygdala activity, increases social interactions, and reduces anxiety-like behavior irrespective of NMDAR antagonism. *Behav. Neurosci.* 2015;129(4):389-98. doi:10.1037/bne0000074.

20.  Raam T, McAvoy KM, Besnard A, Veenema AH, Sahay A. Hippocampal oxytocin receptors are necessary for discrimination of social stimuli. *Nat. Commun.* 2017;8(1):2001. doi:10.1038/s41467-017-02173-0.

21.  Woolley JD, Chuang B, Lam O, et al. Oxytocin administration enhances controlled social cognition in patients with schizophrenia. *Psychoneuroendocrinology* 2014;47:116-125. doi:10.1016/j.psyneuen.2014.04.024.

22.  Davis MC, Lee J, Horan WP, et al. Effects of single dose intranasal oxytocin on social cognition in schizophrenia. *Schizophr. Res.* 2013;147(2-3):393-397. doi:10.1016/j.schres.2013.04.023.

23.  Bartz JA, Zaki J, Bolger N, Ochsner KN. Social effects of oxytocin in humans: context and person matter. *Trends Cogn. Sci.* 2011;15(7):301-9. doi:10.1016/j.tics.2011.05.002.

24.  Leng G, Ludwig M. Intranasal Oxytocin: Myths and Delusions. *Biol. Psychiatry* 2016;79(3):243-250. doi:10.1016/j.biopsych.2015.05.003.

25.  Evans SL, Dal Monte O, Noble P, Averbeck BB. Intranasal oxytocin effects on social cognition: a critique. *Brain Res.* 2014;1580:69-77. doi:10.1016/j.brainres.2013.11.008.

26.  Leppanen J, Ng KW, Tchanturia K, Treasure J. Meta-analysis of the effects of intranasal oxytocin on interpretation and expression of emotions. *Neurosci. Biobehav. Rev.* 2017;78:125-144. doi:10.1016/j.neubiorev.2017.04.010.

27.  Keech B, Crowe S, Hocking DR. Intranasal oxytocin, social cognition and neurodevelopmental disorders: A meta-analysis. *Psychoneuroendocrinology* 2018;87:9-19. doi:10.1016/j.psyneuen.2017.09.022.

28. Gauthier C, Doyen C, Amado I, Lôo H, Gaillard R. [Therapeutic effects of oxytocin in autism: Current status of the research]. *Encephale.* 2016;42(1):24-31. doi:10.1016/j.encep.2015.07.006.

29. Mottolese R, Redoute J, Costes N, Le Bars D, Sirigu A. Switching brain serotonin with oxytocin. *Proc. Natl. Acad. Sci.* 2014;111(23):8637-8642. doi:10.1073/pnas.1319810111.

30. Baskerville TA, Douglas AJ. Dopamine and oxytocin interactions underlying behaviors: Potential contributions to behavioral disorders. *CNS Neurosci. Ther.* 2010;16(3):92-123. doi:10.1111/j.1755-5949.2010.00154.x.

31. Dölen G, Darvishzadeh A, Huang KW, Malenka RC. Social reward requires coordinated activity of nucleus accumbens oxytocin and serotonin. *Nature* 2013;501(7466):179-184. doi:10.1038/nature12518.

32. Yoshida M, Takayanagi Y, Inoue K, et al. Evidence That Oxytocin Exerts Anxiolytic Effects via Oxytocin Receptor Expressed in Serotonergic Neurons in Mice. *J. Neurosci.* 2009;29(7):2259-2271. doi:10.1523/JNEUROSCI.5593-08.2009.

33. Eaton JL, Roache L, Nguyen KN, et al. Organizational effects of oxytocin on serotonin innervation. *Dev. Psychobiol.* 2012;54(1):92-7. doi:10.1002/dev.20566.

34. Lefevre A, Richard N, Jazayeri M, et al. Oxytocin and Serotonin Brain Mechanisms in the Nonhuman Primate. *J. Neurosci.* 2017;37(28):6741-6750. doi:10.1523/JNEUROSCI.0659-17.2017.

35. Kheirouri S, Kalejahi P, Noorazar SG. Plasma levels of serotonin, gastrointestinal symptoms,and sleep problems in children with autism. *Turkish J. Med. Sci.* 2016;46(6):1765-1772. doi:10.3906/sag-1507-68.

36. Lesch K-P. Linking emotion to the social brain. The role of the serotonin transporter in human social behaviour. *EMBO Rep.* 2007;8 Spec No(1S):S24-9. doi:10.1038/sj.embor.7401008.

37. Jørgensen H, Riis ÃM, Knigge ÃU, Kj ÃA, Warberg JÃ. Serotonin Receptors Involved in Vasopressin and Oxytocin Secretion. *J.* 2003;15(19):242-249. Available at: http://onlinelibrary.wiley.com/doi/10.1046/j.1365-2826.2003.00978.x/full.

38. Zhang Y, Damjanoska KJ, Carrasco GA, et al. Evidence that 5-HT2A receptors in the hypothalamic paraventricular nucleus mediate neuroendocrine responses to (-)DOI. *J. Neurosci.* 2002;22(21):9635-42. Available at: http://www.ncbi.nlm.nih.gov/pubmed/12417689.

39. Van de Kar LD, Javed A, Zhang Y, Serres F, Raap DK, Gray TS. 5-HT2A receptors stimulate ACTH, corticosterone, oxytocin, renin, and prolactin release and activate hypothalamic CRF and oxytocin-expressing cells. *J. Neurosci.* 2001;21(10):3572-9. Available at: http://www.ncbi.nlm.nih.gov/pubmed/11331386.

40. Edwards KA, Madden AMK, Zup SL. Serotonin receptor regulation as a potential mechanism for sexually dimorphic oxytocin dysregulation in a model

37

of Autism. *Brain Res.* 2018;1701:85-92. doi:10.1016/j.brainres.2018.07.020.

41. Madden AMK, Zup SL. Effects of developmental hyperserotonemia on juvenile play behavior, oxytocin and serotonin receptor expression in the hypothalamus are age and sex dependent. *Physiol. Behav.* 2014;128:260-269. doi:10.1016/j.physbeh.2014.01.036.

42. McNamara IM, Borella AW, Bialowas LA, Whitaker-Azmitia PM. Further studies in the developmental hyperserotonemia model (DHS) of autism: Social, behavioral and peptide changes. *Brain Res.* 2008;1189:203-214. doi:10.1016/j.brainres.2007.10.063.

43. Raote I, Bhattacharya A, Panicker MM. *Serotonin 2A (5-HT2A) Receptor Function: Ligand-Dependent Mechanisms and Pathways.*; 2007. Available at: http://www.ncbi.nlm.nih.gov/pubmed/21204452.

44. Raote I, Bhattacharyya S, Panicker MM. Functional selectivity in serotonin receptor 2A (5-HT2A) endocytosis, recycling, and phosphorylation. *Mol. Pharmacol.* 2013;83(1):42-50. doi:10.1124/mol.112.078626.

45. Muguruza C, Moreno JL, Umali A, Callado LF, Meana JJ, González-Maeso J. Dysregulated 5-HT2A receptor binding in postmortem frontal cortex of schizophrenic subjects. *Eur. Neuropsychopharmacol.* 2013;23(8):852-864. doi:10.1016/j.euroneuro.2012.10.006.

46. Rasmussen H, Frokjaer VG, Hilker RW, et al. Low frontal serotonin 2A receptor binding is a state marker for schizophrenia? *Eur. Neuropsychopharmacol.* 2016;26(7):1248-50. doi:10.1016/j.euroneuro.2016.04.008.

47. Uhrig S, Hirth N, Broccoli L, et al. Reduced oxytocin receptor gene expression and binding sites in different brain regions in schizophrenia: A post-mortem study. *Schizophr. Res.* 2016;177(1-3):59-66. doi:10.1016/j.schres.2016.04.019.

48. Borroto-Escuela DO, Romero-Fernandez W, Tarakanov AO, et al. Dopamine D2 and 5-hydroxytryptamine 5-HT2Areceptors assemble into functionally interacting heteromers. *Biochem. Biophys. Res. Commun.* 2010;401(4):605-610. doi:10.1016/j.bbrc.2010.09.110.

49. Romero-Fernandez W, Borroto-Escuela DO, Agnati LF, Fuxe K. Evidence for the existence of dopamine d2-oxytocin receptor heteromers in the ventral and dorsal striatum with facilitatory receptor–receptor interactions. *Mol. Psychiatry* 2012;18(8):849-850. doi:10.1038/mp.2012.103.

50. Terrillon S, Durroux T, Mouillac B, et al. Oxytocin and Vasopressin V1a and V2 Receptors Form Constitutive Homo- and Heterodimers during Biosynthesis. *Mol. Endocrinol.* 2003;17(4):677-691. doi:10.1210/me.2002-0222.

51. Felsing DE, Anastasio NC, Miszkiel JM, Gilbertson SR, Allen JA, Cunningham KA. Biophysical validation of serotonin 5-HT2A and 5-HT2C receptor interaction. Vaudry H, ed. *PLoS One* 2018;13(8):e0203137. doi:10.1371/journal.pone.0203137.

52. Łukasiewicz S, Błasiak E, Szafran-Pilch K, Dziedzicka-Wasylewska M.

Dopamine D$_2$ and serotonin 5-HT$_{1A}$ receptor interaction in the context of the effects of antipsychotics - *in vitro* studies. *J. Neurochem.* 2016;137(4):549-560. doi:10.1111/jnc.13582.

53.   de la Mora MP, Pérez-Carrera D, Crespo-Ramírez M, Tarakanov A, Fuxe K, Borroto-Escuela DO. Signaling in dopamine D2 receptor-oxytocin receptor heterocomplexes and its relevance for the anxiolytic effects of dopamine and oxytocin interactions in the amygdala of the rat. *Biochim. Biophys. Acta - Mol. Basis Dis.* 2016;1862(11):2075-2085. doi:10.1016/j.bbadis.2016.07.004.

54.   Ramirez VT, van Oeffelen WEPA, Torres-Fuentes C, et al. Differential functional selectivity and downstream signaling bias of ghrelin receptor antagonists and inverse agonists. *FASEB J.* 2018:fj.201800655R. doi:10.1096/fj.201800655R.

55.   Fuxe K, Borroto-Escuela DO, Tarakanov AO, et al. Dopamine D2 heteroreceptor complexes and their receptor-receptor interactions in ventral striatum: novel targets for antipsychotic drugs. *Prog. Brain Res.* 2014;211:113-39. doi:10.1016/B978-0-444-63425-2.00005-2.

56.   Fuxe K, Borroto-Escuela DO. Volume transmission and receptor-receptor interactions in heteroreceptor complexes: Understanding the role of new concepts for brain communication. *Neural Regen. Res.* 2016;11(8):1220-1223. doi:10.4103/1673-5374.189168.

57.   González-Maeso J, Ang RL, Yuen T, et al. Identification of a serotonin/glutamate receptor complex implicated in psychosis. *Nature* 2008;452(7183):93-7. doi:10.1038/nature06612.

58.   Kolasa M, Solich J, Faron-Górecka A, et al. Paroxetine and Low-dose Risperidone Induce Serotonin 5-HT 1A and Dopamine D2 Receptor Heteromerization in the Mouse Prefrontal Cortex. *Neuroscience* 2018;377:184-196. doi:10.1016/j.neuroscience.2018.03.004.

59.   De la Mora MP, Gallegos-Cari A, Crespo-Ramirez M, Marcellino D, Hansson AC, Fuxe K. Distribution of dopamine D 2-like receptors in the rat amygdala and their role in the modulation of unconditioned fear and anxiety. *Neuroscience* 2012;201:252-266. doi:10.1016/j.neuroscience.2011.10.045.

60.   Wischhof L, Koch M. 5-HT 2A and mGlu2 / 3 receptor interactions : on their relevance to cognitive function and psychosis. 2016:1-11. doi:10.1097/FBP.0000000000000183.

61.   Borroto-Escuela DO, Romero-Fernandez W, Narvaez M, Oflijan J, Agnati LF, Fuxe K. Hallucinogenic 5-HT2AR agonists LSD and DOI enhance dopamine D2R protomer recognition and signaling of D2-5-HT2A heteroreceptor complexes. *Biochem. Biophys. Res. Commun.* 2014;443(1):278-84. doi:10.1016/j.bbrc.2013.11.104.

62.   Brogi S, Tafi A, Désaubry L, Nebigil CG. Discovery of GPCR ligands for probing signal transduction pathways. *Front. Pharmacol.* 2014;5:255. doi:10.3389/fphar.2014.00255.

63.   Borroto-Escuela DO, Li X, Tarakanov AO, et al. Existence of Brain 5-HT1A-5-HT2A Isoreceptor Complexes with Antagonistic Allosteric Receptor-Receptor

39

Interactions Regulating 5-HT1A Receptor Recognition. *ACS omega* 2017;2(8):4779-4789. doi:10.1021/acsomega.7b00629.

64. Schellekens H, Van Oeffelen WEPA, Dinan TG, Cryan JF. Promiscuous dimerization of the growth hormone secretagogue receptor (GHS-R1a) attenuates ghrelin-mediated signaling. *J. Biol. Chem.* 2013;288(1):181-191. doi:10.1074/jbc.M112.382473.

65. Chruścicka B., Wallace Fitzsimons S.E., Druelle C.M., Dinan T.G. SH. Detection and Quantitative Analysis of Dynamic GPCRs Interactions Using Flow Cytometry-Based FRET. *Neuromethods* 2018;140. doi:https://doi.org/10.1007/978-1-4939-8576-0_14.

66. Schellekens H, De Francesco PN, Kandil D, et al. Ghrelińs Orexigenic Effect Is Modulated via a Serotonin 2C Receptor Interaction. *ACS Chem. Neurosci.* 2015;6(7):1186-1197. doi:10.1021/cn500318q.

67. Thyrock A, Stehling M, Waschbüsch D, Barnekow A. Characterizing the interaction between the Rab6 GTPase and Mint3 via flow cytometry based FRET analysis. *Biochem. Biophys. Res. Commun.* 2010;396(3):679-683. doi:10.1016/j.bbrc.2010.04.161.

68. Banning C, Votteler J, Hoffmann D, et al. A flow cytometry-based FRET assay to identify and analyse protein-protein interactions in living cells. *PLoS One* 2010;5(2). doi:10.1371/journal.pone.0009344.

69. Devost D, Zingg HH. Identification of dimeric and oligomeric complexes of the human oxytocin receptor by co-immunoprecipitation and bioluminescence resonance energy transfer. *J. Mol. Endocrinol.* 2003;31(3):461-471. doi:10.1677/jme.0.0310461.

70. Scarselli M, Donaldson JG. Constitutive internalization of G protein-coupled receptors and G proteins via clathrin-independent endocytosis. *J. Biol. Chem.* 2009;284(6):3577-3585. doi:10.1074/jbc.M806819200.

71. Conti F, Sertic S, Reversi A, Chini B. Intracellular trafficking of the human oxytocin receptor: evidence of receptor recycling via a Rab4/Rab5 &quot;short cycle&quot;. *Am. J. Physiol. Endocrinol. Metab.* 2009;296(3):E532-42. doi:10.1152/ajpendo.90590.2008.

72. Di Benedetto A, Sun L, Zambonin CG, et al. Osteoblast regulation via ligand-activated nuclear trafficking of the oxytocin receptor. *Proc. Natl. Acad. Sci.* 2014;111(46):16502-16507. doi:10.1073/pnas.1419349111.

73. Berrada K, Plesnicher CL, Luo X, Thibonnier M. Dynamic interaction of human vasopressin/oxytocin receptor subtypes with G protein-coupled receptor kinases and protein kinase C after agonist stimulation. *J. Biol. Chem.* 2000;275(35):27229-27237. doi:10.1074/jbc.M002288200.

74. Kinsey CG, Bussolati G, Bosco M, et al. Constitutive and ligand-induced nuclear localization of oxytocin receptor. *J. Cell. Mol. Med.* 2007;11(1):96-110. doi:10.1111/j.1582-4934.2007.00015.x.

75. Terrillon S, Cheng LL, Stoev S, Barberis C, Manning M, Durroux T. Synthesis and Characterization of Fluorescent Antagonists and Agonists for Human

Oxytocin and Vasopressin V Receptors Human Oxytocin and Vasopressin V 1a Receptors. *J. Med. Chem.* 2002:2579-2588. doi:10.1021/jm010526.

76. Ward RJ, Pediani JD, Milligan G. Heteromultimerization of cannabinoid CB 1 receptor and orexin OX            1 receptor generates a unique complex in which both protomers are regulated by orexin A. *J. Biol. Chem.* 2011;286(43):37414-37428. doi:10.1074/jbc.M111.287649.

77. Baki L, Fribourg M, Younkin J, et al. Cross-signaling in metabotropic glutamate 2 and serotonin 2A receptor heteromers in mammalian cells. 2016. doi:10.1007/s00424-015-1780-7.

78. Preller KH, Pokorny T, Hock A, et al. Effects of serotonin 2A/1A receptor stimulation on social exclusion processing. *Proc. Natl. Acad. Sci.* 2016;113(18):5119-5124. doi:10.1073/pnas.1524187113.

79. Smith MP, Ayad VJ, Mundell SJ, McArdle CA, Kelly E, López Bernal A. Internalization and Desensitization of the Oxytocin Receptor Is Inhibited by Dynamin and Clathrin Mutants in Human Embryonic Kidney 293 Cells. *Mol. Endocrinol.* 2006;20(2):379-388. doi:10.1210/me.2005-0031.

80. Hasbi A, Devost D, Laporte SA, Zingg HH. Real-Time Detection of Interactions between the Human Oxytocin Receptor and G Protein-Coupled Receptor Kinase-2. *Mol. Endocrinol.* 2004;18(5):1277-1286. doi:10.1210/me.2003-0440.

81. Hanley NRS, Hensler JG. Mechanisms of ligand-induced desensitization of the 5-hydroxytryptamine(2A) receptor. *J. Pharmacol. Exp. Ther.* 2002;300(2):468-77. doi:10.1124/jpet.300.2.468.

82. Jordan BA, Trapaidze N, Gomes I, Nivarthi R, Devi LA. Oligomerization of opioid receptors with beta 2-adrenergic receptors: a role in trafficking and mitogen-activated protein kinase activation. *Proc. Natl. Acad. Sci. U. S. A.* 2001;98(1):343-8. doi:10.1073/pnas.011384898.

83. Lopez-Gimenez JF, Vilaró MT, Milligan G. Morphine desensitization, internalization, and down-regulation of the mu opioid receptor is facilitated by serotonin 5-hydroxytryptamine2A receptor coactivation. *Mol. Pharmacol.* 2008;74(5):1278-91. doi:10.1124/mol.108.048272.

84. Milligan G. A day in the life of a G protein-coupled receptor: The contribution to function of G protein-coupled receptor dimerization. *Br. J. Pharmacol.* 2008;153(SUPPL. 1):216-229. doi:10.1038/sj.bjp.0707490.

85. Borroto-Escuela DO, Romero-Fernandez W, Tarakanov AO, Ciruela F, Agnati LF, Fuxe K. On the existence of a possible A2A-D2-β- arrestin2 complex: A2Aagonist modulation of D2agonist-induced β-arrestin2 recruitment. *J. Mol. Biol.* 2011;406(5):687-699. doi:10.1016/j.jmb.2011.01.022.

86. Luttrell LM, Wang J, Plouffe B, et al. Manifold roles of β-arrestins in GPCR signaling elucidated with siRNA and CRISPR/Cas9. *Sci. Signal.* 2018;11(549). doi:10.1126/scisignal.aat7650.

87. Gimpl G, Reitz J, Brauer S, Trossen C. Oxytocin receptors: ligand binding, signalling and cholesterol dependence. *Prog. Brain Res.* 2008;170(08):193-204. doi:10.1016/S0079-6123(08)00417-2.

41

88. Albizu L, Teppaz G, Seyer R, et al. Toward efficient drug screening by homogeneous assays based on the development of new fluorescent vasopressin and oxytocin receptor ligands. *J. Med. Chem.* 2007;50(20):4976-4985. doi:10.1021/jm061404q.

89. Bonhaus DW, Bach C, DeSouza a, et al. The pharmacology and distribution of human 5-hydroxytryptamine2B (5-HT2B) receptor gene products: comparison with 5-HT2A and 5-HT2C receptors. *Br. J. Pharmacol.* 1995;115(4):622-628. doi:10.1111/j.1476-5381.1995.tb14977.x.

90. Ring RH, Schechter LE, Leonard SK, et al. Receptor and behavioral pharmacology of WAY-267464, a non-peptide oxytocin receptor agonist. *Neuropharmacology* 2010;58(1):69-77. doi:10.1016/j.neuropharm.2009.07.016.

91. Chini B, Manning M. Agonist selectivity in the oxytocin/vasopressin receptor family: new insights and challenges. *Biochem. Soc. Trans.* 2007;35(Pt 4):737-741. doi:10.1042/BST0350737.

92. Bellot M, Galandrin S, Boularan C, et al. Dual agonist occupancy of AT1-R-α2C-AR heterodimers results in atypical Gs-PKA signaling. *Nat. Chem. Biol.* 2015;11(4):271-279. doi:10.1038/nchembio.1766.

93. Reversi A, Rimoldi V, Marrocco T, et al. The oxytocin receptor antagonist atosiban inhibits cell growth via a "biased agonist" mechanism. *J. Biol. Chem.* 2005;280(16):16311-16318. doi:10.1074/jbc.M409945200.

94. Borroto-Escuela DO, Narvaez M, Valladolid-Acebes I, et al. Detection, Analysis, and Quantification of GPCR Homo- and Heteroreceptor Complexes in Specific Neuronal Cell Populations Using the In Situ Proximity Ligation Assay. In: ; 2018:299-315. doi:10.1007/978-1-4939-8576-0_19.

95. Howick K, Alam R, Chruscicka B, et al. Sustained-release multiparticulates for oral delivery of a novel peptidic ghrelin agonist: Formulation design and in vitro characterization. *Int. J. Pharm.* 2018;536(1):63-72. doi:10.1016/j.ijpharm.2017.11.051.
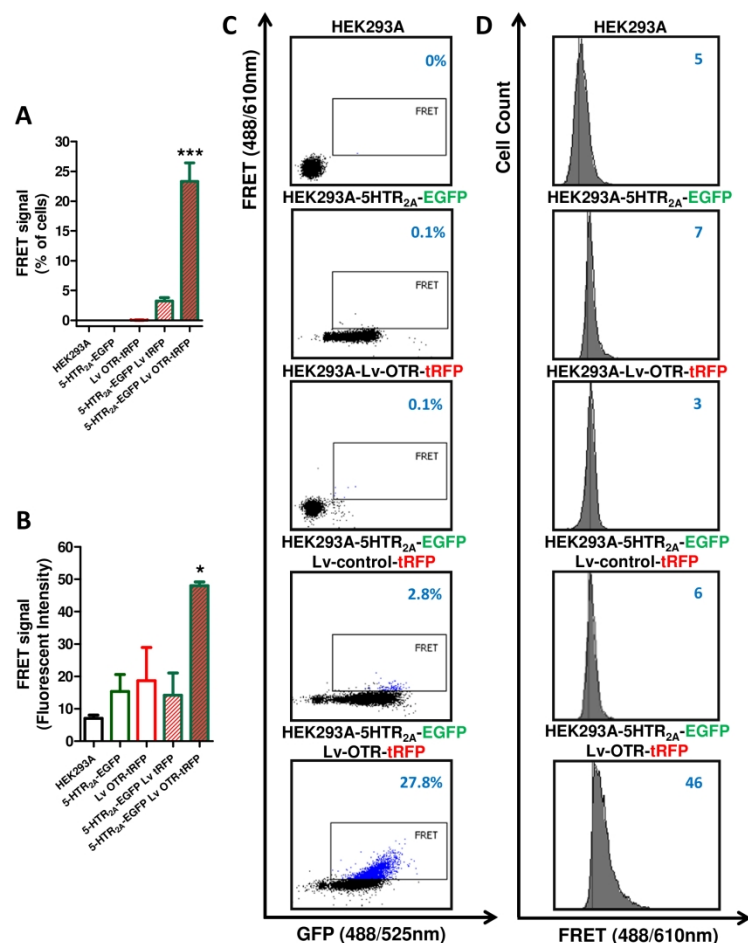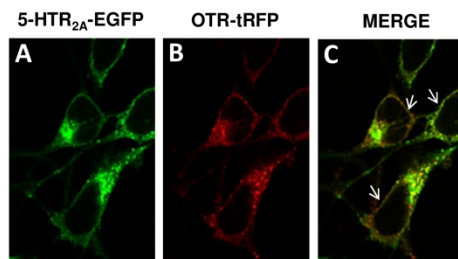
**Figure 1. fcFRET between the OTR and 5-HTR$_{2A}$.** The fcFRET signal is presented as a percentage of cells (A,C) and as median fluorescence (B,D) in wild-type HEK293A cells, cells stably expressing the 5-HTR$_{2A}$ tagged with EGFP (donor), cells transiently transduced with lentiviral vector expressing OTR tagged with tRFP (acceptor), cells expressing 5-HTR$_{2A}$ tagged with EGFP and the control-tRFP, and cells co-expressing 5-HTR$_{2A}$ tagged with EGFP and OTR tagged with tRFP. Graphs represent mean ± SEM from three independent experiments (A,B). Statistical significance of fcFRET signal in cells co-expressing both receptors compared to cells expressing donor with the control acceptor constructs is denoted as * for p < 0.05 and *** for p < 0.001. Dot plots (C) show percentage of cells with fcFRET signal (FRET vs EGFP plots), histograms (D) demonstrate median fluorescence of fcFRET signal (Cell count vs FRET signal). Dot plots and histograms are representative of three independent experiments.
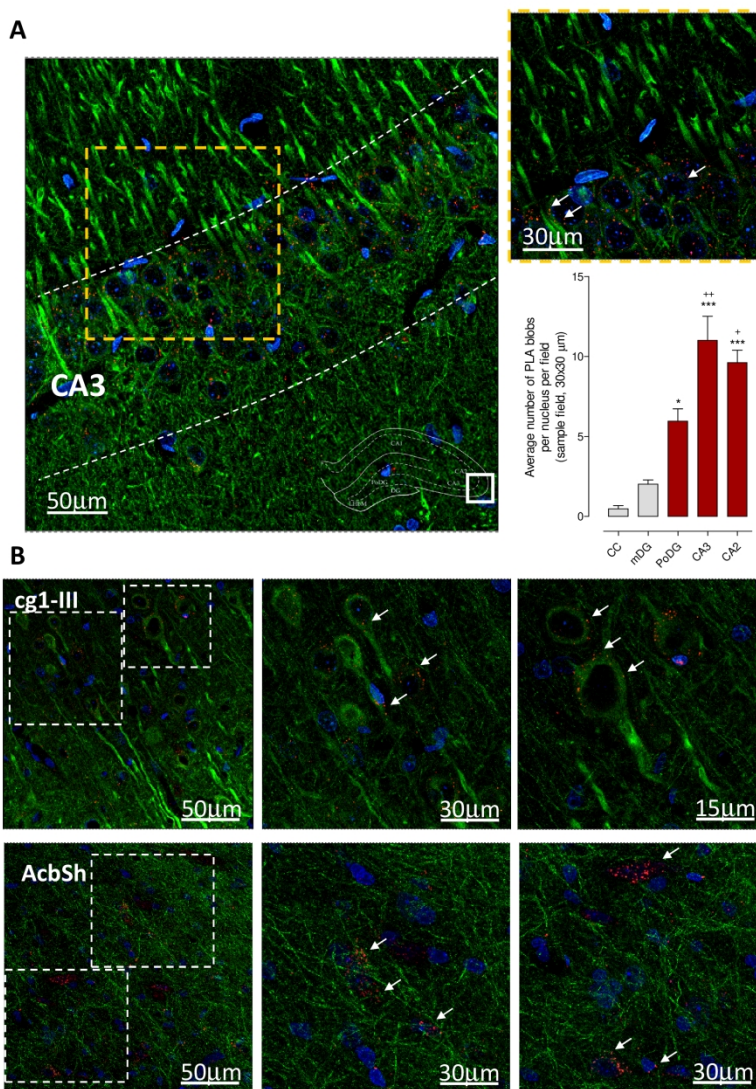
209x297mm (300 x 300 DPI)

1
2
3
4
5
6
7
8
9
10
11
12
13
14
15
16
17
18
19
20
21
22
23
24
25
26
27
28
29
30
31
32
33
34
35
36
37
38
39
40
41
42
43
44
45
46
47
48
49
50
51
52
53
54
55
56
57
58
59
60

**Figure 2. Cellular colocalization of the OTR/5-HTR$_{2A}$ pair.** HEK293A cells stably expressing the 5-HTR$_{2A}$ tagged with EGFP (green) (A) were transiently transduced with lentiviral vector expressing OTR tagged with tRFP (red) (B). Merged picture (yellow/orange) shows colocalization of the two receptors within the cell (C).

209x297mm (300 x 300 DPI)

**Figure 3. Illustration of the OTR-5HTR$_{2A}$ heteroreceptor complexes in the dorsal hippocampus and nucleus accumbens of rat brain.** Microphotographs from transverse sections of the rat dorsal hippocampus (Bregma level: -3.6 mm) show the distribution of the OTR-5HTR$_{2A}$ heteroreceptor complexes in CA3 using the in situ proximity ligation assay (in situ PLA) technique. The square outlines the CA3 area from which the picture was taken. Receptor complexes are shown as red PLA blobs (clusters) found in high densities per cell in a large number of nerve cells in the pyramidal cell layer using confocal laser microscopy. No specific PLA blobs were found in the stratum moleculare and radiatum of the CA3-CA2 regions (cornus ammonis). The nuclei are shown in blue by DAPI staining and the neuronal marker in green. In the higher right panel the PLA blobs are presented in higher magnification in the pyramidal cell layer. In the lower right part of the figure the density (per nucleus per sampled field) of the PLA positive complexes in PoDG (polymorph layer of the dentate gyrus), CA3, and CA2 are highly significantly different (***) from the density found in crus cerebri (CC) and the granular cell layer of the dentate gyrus (gDG). The density is also significantly higher in the CA2 (+) and CA3 (++) versus PoDG (Mean ± SEM, 4 rats per group) (A). The

1
2
3
4
5
6
7
8
9
10
11
12
13
14
15
16
17
18
19
20
21
22
23
24
25
26
27
28
29
30
31
32
33
34
35
36
37
38
39
40
41
42
43
44
45
46
47
48
49
50
51
52
53
54
55
56
57
58
59
60

upper panel of B show representative examples of these PLA receptor complexes from transverse sections of the rat cingulate cortex, area 1 (Bregma level: 1.2 mm). They present the distribution of OTR-5HTR$_{2A}$ heteroreceptor complexes. They are shown as red PLA blobs (clusters) with high densities in layer III and low to moderate densities in layer II. Layer III represents the external pyramidal cell layer where large PLA positive clusters are found and appear to be located on the surface of many pyramidal cells. Higher magnifications of the two squares outlined in left panel are shown in the two right panels. The nerve cell bodies and apical dendrites are seen in green (neuronal marker). The lower panel in B is taken from nucleus accumbens shell (AcbSh). The neuronal marker (Neuro-Chrom$^{TM}$ Pan neuronal marker antibody-Alexa488 conjugated, ABN2300A4) shows the neurite network. Discrete nerve cell bodies are associated with a high density of PLA positive blobs representing OTR-5HTR$_{2A}$ heteroreceptor complexes that may also have an intracellular location through trafficking. The outlined squares in the left panel are shown in higher magnifications in the two right panels (B).
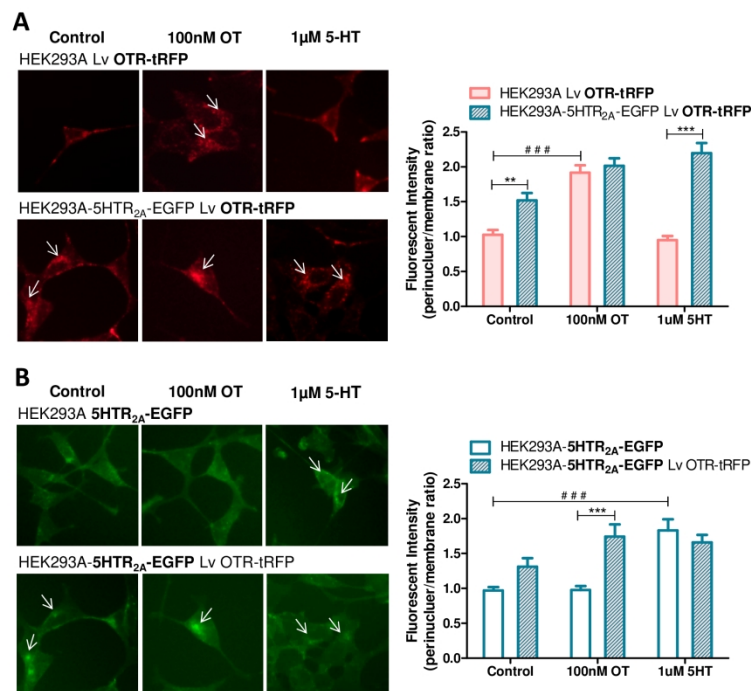
209x297mm (300 x 300 DPI)

**Figure 4. Cellular trafficking of the OTR and 5-HTR$_{2A}$.** Representative images (left panel) and quantitative analysis (right panel) of ligand-mediated internalization of OTR tagged with tRFP (A) and 5-HTR$_{2A}$ tagged with EGFP (B) versus cells co-expressing both receptors. Graphs represents mean ± SEM from three independent experiments run in triplicate. Statistical significance of cells co-expressing both receptors compared to cells solely expressing the corresponding receptor is denoted as; ** indicating $p < 0.01$; or *** indicating $p < 0.001$. Statistical significance of cells following OTR or 5-HT treatment compared to the control condition is denoted as; # # # indicating $p < 0.001$.
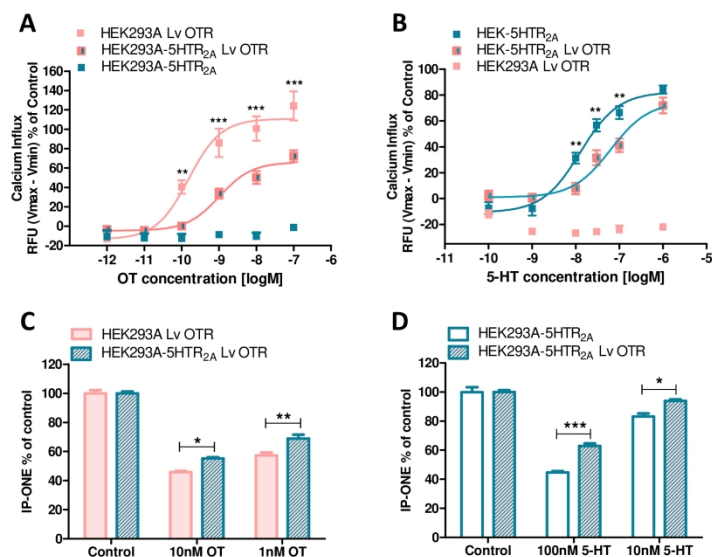
209x297mm (300 x 300 DPI)

**Figure 5. Co-expression of the OTR and 5-HTR$_{2A}$ attenuates G$\alpha$q-dependent signalling of both receptors.** Intracellular calcium release induced by increasing concentration of OT (A) and 5-HT (B) in HEK293A cells stably expressing the 5-HTR$_{2A}$ tagged with EGFP, in cells transiently expressing OTR tagged with tRFP, and in cells co-expressing both receptors. Intracellular calcium mobilization is presented as a percentage of maximal calcium response elicited by the control (3% FBS). Graphs represent means ± SEM from at least three independent experiments run in triplicates. IP-One production induced by 10 nM and 1 nM OT (C), and 100 nM and 10 nM 5-HT (D) in HEK293A cells stably expressing 5-HTR$_{2A}$ tagged with EGFP, in cells transiently expressing OTR tagged with tRFP, and in cells co-expressing both receptors. IP-One production is presented as a percentage of control (100% for non-stimulated cells). Graphs represent means ± SEM from experiments run in triplicate. Statistical significance of cells co-expressing both receptors compared to cells solely expressing one receptor is denoted as * for $p < 0.05$, ** for $p < 0.001$, and *** for $p < 0.001$.

209x297mm (300 x 300 DPI)

1
2
3
4
5
6
7
8
9
10
11
12
13
14
15
16
17
18
19
20
21
22
23
24
25
26
27
28
29
30
31
32
33
34
35
36
37
38
39
40
41
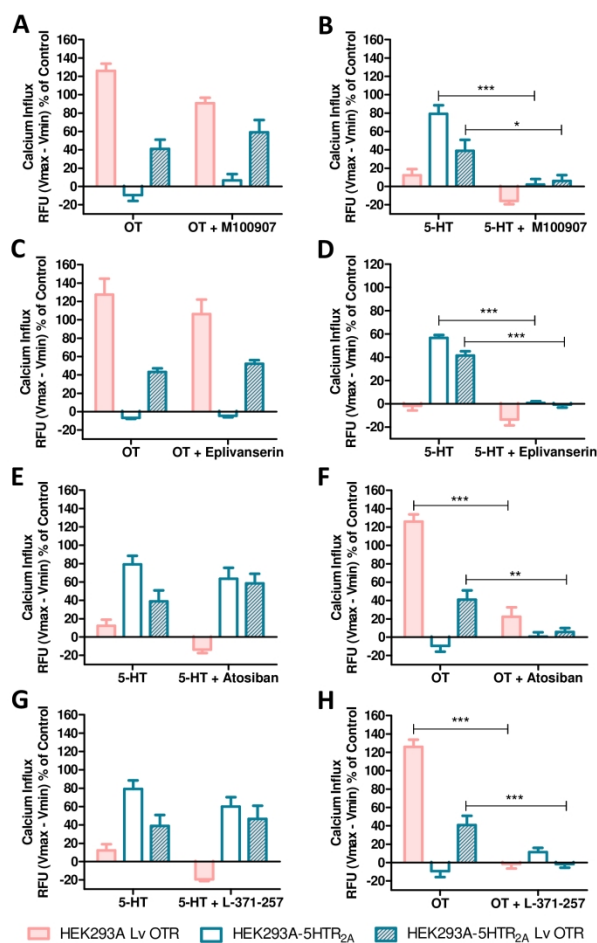42
43
44
45
46
47
48
49
50
51
52
53
54
55
56
57
58
59
60

**Figure 6. Pharmacological inhibition of the OTR or 5-HTR$_{2A}$ does not affect the OTR–5-HTR$_{2A}$ heterocomplex specific Gαq-dependent signalling.** Intracellular calcium release in cells solely expressing OTR, cells solely expressing 5-HTR$_{2A}$, and cells co-expressing both receptors induced by 10 nM OT alone and in the presence of 1 μM 5-HTR$_{2A}$ antagonists; M100907 (A) and Eplivanserin (C), as well as 1 μM OTR antagonists; Atosiban (F) and L-371-257 (H). Intracellular calcium release induced by 100 nM 5-HT alone and in the presence of 1 μM OTR antagonists; Atosiban (E) and L-371-257 (G), as well as 5-HTR$_{2A}$ antagonists; M100907 (B) and Eplivanserin (D). All graphs represent means ± SEM from at least two independent experiments run in triplicates, demonstrated as percentage of maximum calcium response (3% FBS). Statistical significance of cells co-expressing both receptors compared to cells solely expressing corresponding receptor is denoted as * for $p < 0.05$, ** for $p < 0.001$, and *** for $p < 0.001$.

209x297mm (300 x 300 DPI)

1
2
3
4
5
6
7
8
9
10
11
12
13
14
15
16
17
18
19
20
21
22
23
24
25
26
27
28
29
30
31
32
33
34
35
36
37
38
39
40
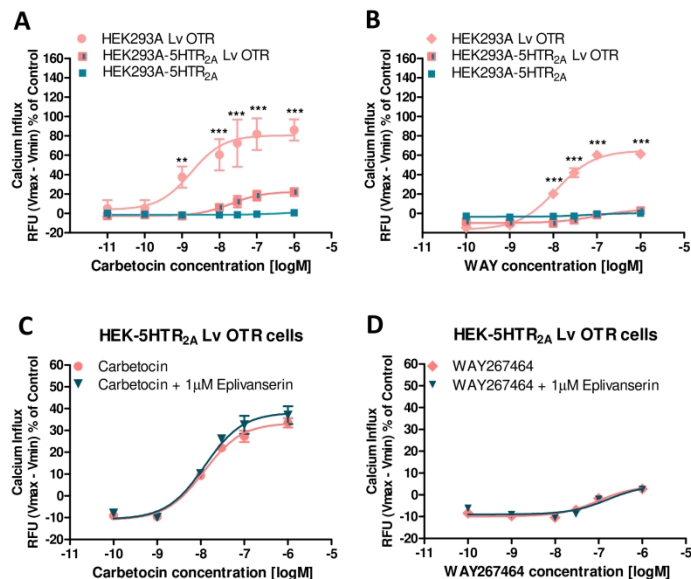41
42
43
44
45
46
47
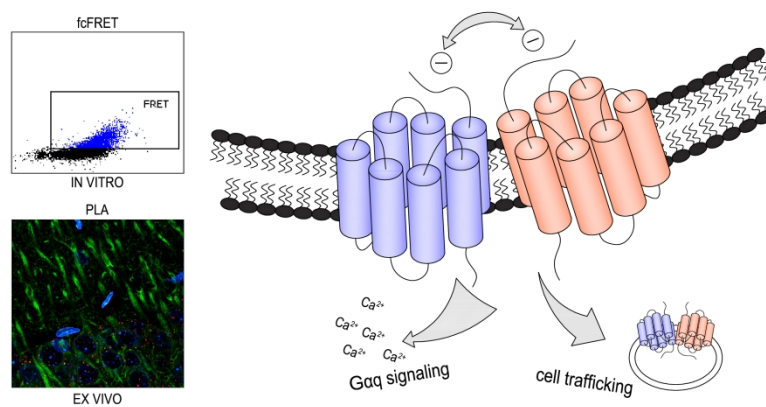48
49
50
51
52
53
54
55
56
57
58
59
60

1
2
3
4
5
6
7
8
9
10
11
12
13
14
15
16
17
18
19
20
21
22
23
24
25
26
27



28
29
30
31
32
33
34
35
36
37
38
39
40
41
42
43
44
45

Figure 7. Synthetic OTR ligand-mediated attenuation of Gαq-dependent signalling in cells co-expressing the OTR and 5-HTR$_{2A}$. Intracellular calcium release induced by increasing concentration of Carbetocin (A) and WAY265464 (B) in cells expressing OTR, in cells expressing 5-HTR$_{2A}$, and in cells co-expressing both receptors. Graphs present mean ± SEM from et least two independent experiments run in triplicates. Statistical significance of cells co-expressing both receptors compared to cells solely expressing corresponding receptor is denoted as ** for $p < 0.001$, and *** for $p < 0.001$. Intracellular calcium release induced by increasing concentration of Carbetocin (C) and WAY (D) in the presence of 5-HTR$_{2A}$ antagonist; Eplivanserin in cells co-expressing both receptors. Graphs present mean ± SEM from an experiment run in triplicate. Results are demonstrated as a percentage of maximum calcium response (3% FBS).

209x297mm (300 x 300 DPI)

Graphical table of contents